Anonymous Referee #1

General comments

This paper describes the leaf phenology scheme of the Ent model and aims to identify sources of error in the model structure and parameterization through a number of experiments. This is an interesting and timely question as phenology is a key component of land surface models which is as yet not well represented in any of the existing models. Furthermore, identifying sources of error in complex vegetation models is often difficult so the experimental approach taken by the authors is a very useful tool and should be employed in more modeling studies. The discussion of errors created by both phenology and biomass allocation is valuable as timing of growth and pattern of growth are often discussed separately despite the obvious close link between them.

The phenology scheme used by Kim et al aims to capture cold deciduous phenology, seasonally dry phenology and cold evergreen photosynthesis seasonality. The three components are a combination of parametrisations from other studies and it is not clear to me why the authors did not choose to use either a new parametrisation or a whole scheme from another study such as Jolly et al. (2005) or Caldararu et al. (2014). Having said that, the entire Ent model appears to be made out of components of other models and studies so maybe this is a larger question, not specific to this paper.

The idea behind the phenology scheme appears to be that we do not have a mechanistic understanding of phenology and cannot therefore build a process-based model (p.5819, line 25). This is not strictly true as a large number of plant sciences studies as well as some biogeosciences ones more recently, have tried to understand the physiological drivers behind leaf seasonality. In addition, recent modelling studies are trying to move towards models that incorporate our understanding of plant and ecosystem processes (Prentice et al., 2015; Norby et al., 2015).

The paper is generally well written, with the exception of the introduction, which is lengthy and a bit sloppy. Some of the introduction material can be found in the methods, while some of the methods material can, mysteriously, be found in the results section.

Overall, the Ent phenology model is correct and the results revealed by the experiments undertaken in this paper are interesting and should be applied more widely in the modelling community but the introduction needs re-writing and some of the model assumptions need clarification and justification.

Specific comments

>> We would like to express our appreciation to the reviewer for a very close, thoughtful, and helpful review.

>> In response to the reviewer's comment that the introduction/methods/results are not clearly separated, we have rearranged to fix this.

p 5810 line 23 The first sentence seems incomplete. Saying "these models" implies to me that there is maybe a sentence missing.

>> Please be advised that a mistake in the copyediting process led the incomplete sentence in the beginning of the manuscript. We have corrected it.

In the 1st paragraph of *1. Introduction* of the revised manuscript:
Phenological timing remains a major weakness of land surface dynamic global vegetation models (DGVMs) that are coupled to general circulation models (GCMs), and a primary cause of uncertainty in predicting the trajectory of global atmospheric CO2 (Friedlingstein et al. 2006, Friedlingstein et al. 2014).

p 5811 line 17 I would suggest deleting or shortening this paragraph, there are a lot of examples here in addition to the ones in the previous paragraph.

>> As per reviewer's suggestion, we have shortened the paragraph with deleting abundant literature reviews.

In the 2nd paragraph of *1. Introduction* of the revised manuscript:
Given the strong interactions between phenology and other land surface and ecosystem processes, phenology affects both weather and climate. Seasonal variation in vegetation characteristics have been shown to significantly influence summer precipitation and temperature in the U.S. (Dirmeyer 1994, Xue et al. 1996), and enhance or weaken the feedbacks between soil moisture and precipitation in the continental interior of North America depending on soil moisture conditions and season (Kim and Wang 2007). Levis and Bonan (2004) demonstrated that the coupling between phenology and the atmosphere is critical for models to capture seasonal weather evolution. Tightly linked to phenology, plant carbon allocation, that is, distribution of assimilated carbon among the plant parts, also responds to environmental and climate conditions (such as increases in air temperature, changes in precipitation patterns and elevated atmospheric CO2 concentration). For example, Pumpanen et al. (2012) observed that root biomass and the rate of photosynthesis for silver birch, Norway spruce and Scots pine seedlings increase with higher soil temperature, yet a simultaneous increase in both photosynthesis and respiration rates results in no change in net CO2 exchange and total seedling biomass.

p 5812 line 13 This sentence suggests that the main purpose of coupling DGVMs with GCMs is to represent phenology.

>> We have re-written the sentence to clarify the meaning.

In the 3rd paragraph of *1. Introduction* of the revised manuscript:
Terrestrial biosphere models (TBMs) or Dynamic Global Vegetation Models (DGVMs) have been developed and coupled to General Circulation Models (GCMs) (e.g., Foley et al. 1996, Cox 2001, Sitch et al. 2003, Bonan and Levis 2006, Dunne et al. 2013), to account for biophysical and biogeochemical processes and sometimes biogeography, allowing prediction of transient terrestrial ecosystem interactions with climate (Cramer et al. 2001, Friedlingstein et al. 2006). Thus the active role of vegetation phenology can be incorporated into climate modeling.

p 5813 line 12 Again, you might want to shorten this paragraph, the introduction is meant to set the stage for the model, not provide a full review of the Richardson papers.

>> We have shortened the review on the Richardson paper and moved it to the phenology subsection.

In the 2nd paragraph of *2.4. Phenology* of the revised manuscript:
Furhtermore, Richardson et al. (2012) conducted an inter-comparison of phenology predictions of eleven TBMs (and three biophysics models with prescribed phenology) at five deciduous broadleaf and five evergreen needleleaf Fluxnet sites. They found that, for deciduous forests, most consistently predicted an earlier onset of the growing season and later fall senescence than observed; meanwhile, most models under-predicted the magnitude of peak GDD sums, while those that explicitly or implicitly included a chilling requirement did relatively well in capturing the onset of LAI and GPP for deciduous and evergreen forests, compared to simple temperature threshold schemes.

p 5814 line 2 You might want to move the version enumeration to either the methods or the footnote with the wonderful Tolkien comment, which made me laugh.

>> As per reviewer's suggestion, we have moved the version enumeration to the footnote.

In the footnote of *1. Introduction* of the revised manuscript:
[2] Enumeration is in order for different levels of dynamics and different physics versions available for each of these. In order, the digits denote:
1) Primary biophysics (leaf, soil biogeochemistry) and base release version (1: leaf biophysics as described in Schmidt et al. 2014; soil biogeochemistry described in this paper).
2) Canopy radiative transfer (0: two-stream as described in Schmidt et al. 2014; 1: ACTS model (Ni-Meister et al. 2010; Yang et al., 2010);
3) Leaf phenology (0: prescribed from satellite data; 1: prognostic, this paper);
4) Carbon allocation/growth (0: allocation with prognostic phenology, without structural growth, this paper; 1: allocation with structural growth).
5) Ecosystem dynamics (0: none; 1: Ecosystem Demography scheme).

p 5819 line 24 - p 5821 line 18 All this material belongs in the introduction and might need shortening.

>> As per reviewer's suggestion, we have re-written the paragraphs and also rearranged with moving two of these paragraphs into the part of introduction section.

In the 4th and 5th paragraph of *1. Introduction* of the revised manuscript:
Prognostic phenology models have been developed to predict phenological response of vegetation to climate based on empirical evidence, as a mechanistic, process-based treatment is still not fully realizable with current understanding (Sala et al. 2012). The commonly used climatic rule-based approach accounts for temperature, soil moisture, and day length cues to phenology, to predict leaf-on and leaf-off, with these controls often represented as a cumulative functions of one or several climate variables that reach an empirically defined threshold (White et al. 1997). Another approach is based on plant carbon status (Bonan et al.

2003), and predicts leaf-out and senescence on the basis of potential positive carbon assimilation, which is in turn is affected by temperature, moisture, and sometimes nutrient conditions.

All of the above approaches require empirical parameterization of the responses to climate, and a model scheme that is independent of PFT or geographical variation is still a research goal. Jolly et al. (2005) have proposed a very simple and promising bioclimatic Growing Season Index (GSI) for phenology based on linear relations to minimum temperature, photoperiod, and vapor pressure deficit (VPD, as a proxy for soil moisture), which seems to perform well compared to satellite observations at diverse sites. However, it performs less well for arid systems for which VPD may not be a good indicator of available deep soil moisture, and it is not able to capture any seasonal moisture or light sensitivity that has been observed in tropical evergreen forests (Stockli et al. 2011). Forkel et al. (2014) adopted the concept of GSI but used the soil water availability instead of VPD for water limiting function. Phenology depends not only on atmospheric water demand but also on water supply from soil moisture as Migliavacca et al. (2011) have shown that GSI performed better when using a soil moisture limiting function instead of the VPD limiting function. Recently, Caldarau et al. (2014) introduced a promising optimality approach based on the hypothesis that phenology is a strategy for optimal leaf area index, rather than explicit carbon exchange, driven by canopy-level demand for – and constrained by availability of -- light and water, limited by leaf aging. They fitted the model to satellite observations of LAI and demonstrated its capability to reproduce phenological patterns for different vegetation types over the globe within 8-16 days of observations.

In the 1ˢᵗ and 2ⁿᵈ paragraph of *2.4. Phenology* of the revised manuscript:

The phenology scheme in the Ent TBM provides a synthesis, and combines the climatic rule-based approach and carbon balance for deciduous plants to determine the timings and rates of leaf out and leaf senescence by integrating several different modeling studies. We present a diversity of PFTs, adding those with known behaviors that depart from common representations of cold, drought, or light responses. While globally applicable parameterizations of climate rule-based phenology may still be elusive, where available in the literature, we draw from wide surveys that attempt to extrapolate to the global scale.

For deciduous plants, we use parameterizations by Botta et al. (2000). With growing degree day (GDD) and chilling requirement, they examined the possibility of extrapolating existing local models for leaf onset date to the global scale by retrieving leaf onset dates from the NOAA/AVHRR satellite normalized difference vegetation index (NDVI). They identified appropriate leaf onset date models and estimated their parameters for each biome, which are implemented in other ecosystem models (Medvigy et al. 2008). The importance of a chilling requirement is confirmed by Richardson et al. (2012), who conducted an inter-comparison of phenology predictions of eleven TBMs (and three biophysics models with prescribed phenology) at five deciduous broadleaf and five evergreen needleleaf Fluxnet sites. They found that, for deciduous forests, the models consistently predicted an earlier onset of the growing season and later fall senescence than observed; meanwhile, most models under-predicted the magnitude of peak GDD sums, while those that explicitly or implicitly included a chilling requirement did relatively well in capturing the onset of LAI and GPP for deciduous and evergreen forests, compared to simple temperature threshold schemes. For drought deciduous trees and grasses, we also make use of parameterizations of White et al. (1997) who developed a regional phenology model for the US, predicting timings of leaf onset

and offset based on the satellite NDVI at the 20 km resolution. Their prediction errors are ~1 week, and maximum expected errors are 10-14 days.

p 5819 line 24 As I said above, this statement is not strictly true and since it forms the basis of the chosen phenology scheme you should at least justify it a bit more.

>> As per reviewer's suggestion, we have re-written the sentence to clarify it as specific to our climate rule-based approach. If we may, we would like to interpret the approach of Caldararu et al. (2014) as an optimality, top-down constraint-based approach, rather than mechanistic process-based. Rather than simulating leaf level physiology or biochemical processes, they are integrating whole canopy demand for light and water scaled by leaf area index, and this is actually independent of explicit carbon exchange (so it is not actually a carbon optimality model, but LAI optimality model). We are glad to learn of this paper from Reviewer 1, and are quite impressed by their concept and its fairly consistent performance globally. We would like to observe that the independence from carbon exchange may in fact be consistent with the work of Osnas et al. (2013) on leaf mass vs. area traits, in which many traits scale by area, while leaf thickness seems to distinguish species tradeoff strategies. The next challenge is to integrate the leaf area timing of Caldararu et al. (2014) with carbon exchange and allocation. So, we still maintain that a mechanistic understanding of phenology is still elusive, but as phenology is in a sense a strategic behavior of plants, it may make good sense for models to replace the mechanistic approach with an optimality strategy instead (e.g. ecohydrological optimality theory of Rodriguez-Iturbe, Porporato, and co-workers, and a hedging model of co-author Kiang in the last chapter of her dissertation).

In the 4th paragraph of *1. Introduction* of the revised manuscript still states:
Prognostic phenology models have been developed to predict phenological response of vegetation to climate based on empirical evidence, as a process-based treatment is still not fully realizable with current understanding (Sala et al. 2012).

However, in the 6th paragraph of *1. Introduction* of the revised manuscript, we add:
Recently, Caldararu et al. (2014) introduced a promising optimality approach based on the hypothesis that phenology is a strategy for optimal leaf area index, rather than explicit carbon exchange, driven by canopy-level demand for – and constrained by availability of -- light and water, limited by leaf aging. They fitted the model to satellite observations of LAI and demonstrated its capability to reproduce phenological patterns for different vegetation types over the globe within 8-16 days of observations. Top-down optimality approaches such as this may indeed be the smart way for global scale models way to capture the strategic behaviors inherent in phenology in lieu of mechanistic understanding at the leaf or molecular level; the next step remains to couple them with explicit carbon exchange and allocation.

p 5820 line 15 You might want to mention that the Jolly et al. (2005) scheme has been implemented into a DGVM with good results by Forkel et al. (2014).

>> As per reviewer's suggestion, we have added additional explanation relevant to Jolly et al.'s scheme.

In the 2nd paragraph of *2.4 phenology* of the revised manuscript:

Forkel et al. (2014) adopted the concept of GSI but used the soil water availability instead of VPD for water limiting function. Phenology depends not only on atmospheric water demand but also on water supply from soil moisture as Migliavacca et al. (2011) have shown that GSI performed better when using a soil moisture limiting function instead of the VPD limiting function.

p 5820 line 21 See Caldararu et al. (2014) for a globally applicable phenology model.

>> As per reviewer's suggestion, we have acknowledged Caldararu's fairly robust results at the global scale in the Introduction, and more precisely noted that is the climate rule-based approach that has difficulty with global scale parameterizations.

In the 1st paragraph of *2.4 phenology* of the revised manuscript:
While globally applicable parameterizations of climate rule-based phenology may still be elusive, where available in the literature, we draw from wide surveys that attempt to extrapolate to the global scale.

p 5821 line 19 What is the relationship between Phenostatus and the various φ factors? Are they the same thing? How do you put everything together? A master equation at this stage would be very helpful.

>> We have re-written this part of paragraphs as the original manuscript included some misleading sentences. We have put the description of "phenological factors" and *Phenostatus*, as well as day length, *ld*, in a sub-section "2.4.1 Phenology Model Climate Cue Framework," to make the organization clearer. *Phenostatus* is an indicator for different phenological phases of no-leaf (1), leaf onset (spring) (2), full leaf (3) and leaf offset (fall) (4).

In the two paragraphs of *2.4.1 phenology Model Climate Cue Freamework* of the revised manuscript:
In the Ent TBM, several "phenological factors", ϕ_x, as well as physiological stress factors, β_x, are calculated for seasonal environmental cues from various climate measures x. These include air and soil temperature history (cumulative number of growing degree days and of chilling days), day-length and soil moisture. The phenological factors control the allocation of assimilated carbon, while the physiological stress factors affect the efficiency of carbon uptake, and all range from 0 to 1 on a daily basis. Different rules apply to the different PFTs, according to phenotype (woody plant cold-deciduous, cd, drought-deciduous, dd, evergreen, ev, tropical radiation phenology, tr; and cold deciduous herbs, c, whether annual or perennial). The phenological factor controls the timing and rate of carbon transfer between the labile and active carbon pools and hence the seasonal variation in leaf area index (LAI), fine roots, and sapwood.
Furthermore, the Ent TBM determines "phenological status", Phenostatus$_p$, where p is the phenotype, which identifies phenologically different seasons. For plants with seasonal leaf-out and senescence, Phenostatus$_p$ is 1 for the leaf-off season, 2 for the leaf-up period, 3 for the peak foliage period, and 4 for the senescent period. The trend in length of day (ld) is used to determine which season it is, or, rather, which half of the year it is. If day length is decreasing, then it is the latter half of the year, and "fall" may be allowed to commence, depending on other climate variables of phenological factors. Below we itemize these variables and equations in the Ent phenology scheme.

p 5822 line 10 Generally, it is considered that photoperiod plays a much bigger role in leaf phenology, especially in spring and this simple approach you have chosen needs to be justified more.

>> We have re-written the paragraph as the original manuscript included some misleading sentences. This part simply explains how we used the photoperiod for determining *Phenostatus* (for determining whether it is spring or fall). Indeed, as in Eq. (5), we have considered the photoperiod as a critical factor for determining phenological factor ϕ.

In the last paragraph of *2.4 phenology* of the revised manuscript:
Furthermore, the Ent TBM determines "phenological status", Phenostatus$_p$, where p is the phenotype, which identifies phenologically different seasons. For plants with seasonal leaf-out and senescence, Phenostatusp is 1 for the leaf-off season, 2 for the leaf-up period, 3 for the peak foliage period, and 4 for the senescent period. The trend in length of day (ld) is used to determine which season it is, or, rather, which half of the year it is. If day length is decreasing, then it is the latter half of the year, and "fall" may be allowed to commence, depending on other climate variables of phenological factors. Below we itemize these variables and equations in the Ent phenology scheme.

p 5822 line 20 How did you choose the 5o C base temperature? What about the 10 day running average?

>> We have added the reference, Kim and Wang (2005).

p 5822 eq. 1 This equation does not make any sense. Do you mean sum of maximum? Also, the sum must be from something to something. Do you actually mean:

$$GDD(t) = \sum_{t=1}^{t} max(0, T_{10} - T_{base})$$

p 5822 eq. 2 You probably want to format this as above and get rid of the if.
p 5823 eq. 4 Do you mean GDD higher than GDDcrit ? Otherwise your index goes from -1 to zero.

>> We have corrected the equations 1, 2 and 4 as follows:
Follwing Kim and Wang (2005), the 10-day running average of air temperature (T_{10}) difference from the base temperature (T_{base}) of 5℃ is used to calculate GDD and NCD on a daily basis as follows:
$$GDD(t) = GDD(t-1) + max(0, T_{10} - T_{base}) \qquad (1)$$
$$NCD(t) = NCD(t-1) + 1 \ \ if \ \ T_{10} < T_{base}. \qquad (2)$$
where t is time in days. GDD and NCD are reset to be zero at the beginning of the winter season (when Phenostatus$_{cd}$ switches from 4 to 1).
...
We introduce an approach to scale the departure of GDD from GDD$_{crit}$ with GDD$_{length}$, and to have a phenology factor, φ_{GDD}, that ranges from 0 to 1:
$$\varphi_{GDD} = \begin{cases} \frac{GDD - GDD_{crit}}{GDD_{length}} & when \ \ GDD > GDD_{crit}, \\ 0 & otherwise. \end{cases} \qquad (4)$$

p 5825 section 2.4.4 What are the drivers for leaf on in seasonally dry systems?

>> To clarify the meaning, we have re-written the sentence.

In *2.4.3. Drought deciduous woody and herbaceous plants* of the revised manuscript:
Drought deciduousness depends on available soil water for the plant. In the model, it is determined based on a 10-day running average of the physical time step (~half-hourly) plant water stress factor β.
....
The leaf-on cue for drought deciduous trees is the same as that for cold-deciduous trees, while for grasses the cue is sufficient soil moisture.

p 5828 line 18 I do not understand how in your allocation scheme when the leaves have just started growing so that the LAI is very low, there is enough carbon available for a sudden jump to maximum LAI.

>> In general, reserve carbon stores in trees are sufficient to grow maximum LA per plant. In herb seeds, we use a rule of thumb from Bill Parton (pers. Communication) that the carbon store is about 4 times that needed for the max LA of the plant. We have re-written the sentence as follows:

In *4.1.1. Phenology* of the revised manuscript:
First, it is clear that the gradual nature of changes in LAI during spring and fall were not captured in the model. The phenological factor serves as an on-/off cue between environmental thresholds, while growth rate with the ED scheme is limited only by carbon availability, for which reserve carbon is generally not limiting in trees (Sala et al. 2012) or in grass seeds (William Parton, personal communication).

p 5830 line 5 Information about the sites belongs in the methods section.
p 5832 line 12 Again, this belongs in the methods.

>> To describe the site data, we have written a separate subsection of 3.1. Fluxnet sites.

In *3.1. Fluxnet sties* of the revised manuscript:
        The Ent TBM was evaluated at five Fluxnet sites, including Morgan Monroe State Forest, Harvard Forest, the Vaira Ranch, the Tonzi Ranch and Hyytiala, as briefly mentioned above (Table 3).   From all sites, data from the flux tower systems were available. Meteorological driver data include radiation, precipitation, air temperature, air pressure, humidity and wind, used to drive the model.   Soil moisture and temperature measurements were also used to drive the Ent standalone simulations. Flux data includes net ecosystem exchange (NEE) and evapotranspiration (ET), and were used to evaluate the simulation results. Among sites, data availability, such as LAI, varied and suited different types of model simulations as described in detail in the next section.
        The Morgan Monroe Sate Forest (MMSF), located in Indiana, USA (Schmid et al., 2000) (latitude: 39.32315°, longitude: -86.413139°) is is an extensive managed temperate broadleaf deciduous forest with a total area of 95.3 km^2. The area is covered primarily by a secondary successional broadleaf forest within the maple-beech to oak-hickory transition zone of the eastern deciduous forest, dominated by supar maple and tuilip poplar. LAI measurements at 5-14 day intervals during the growing season were available for 1998-2001.

Harvard Forest (latitude: 42.5313°, longitude: -72.1898°) is an eastern temperate mixed forest dominated by deciduous trees. The area surrounding the flux tower is dominated by red oak and red maple, with scattered stands of Eastern hemlock, white pine and red pine. About 1/3 of the existing red oaks were established prior to 1895, another 1/3 prior to 1930, and the rest before 1940, and thus the stand is 75–110 years old (Urbanski et al., 2007). O'Keefe (2000) provides the leaf phenology of Harvard Forest. The timings of spring leaf development and fall leaf fall have been recorded for permanently tagged individuals in the field from 1991. The leaf development and senescence data in percent of final leaf size have been used to obtain 'observational' LAI based on the maximum LAI in the model, i.e., (observed LAI) = (observed % of leaf development or fall) X (modeled maxmimum LAI).

The Vaira Ranch (latitude: 38.4066667°, longitude: -120.950733°) and Tonzi Ranch (latitude: 38.4316°, longitude: -120.9660°) in Ione, California, are located in an open grassland ecosystem and an oak/grass savanna ecosystem, respectively, in a Mediterranean climate of cool wet winters, and dry hot summers. The sites are less than 3 km apart. The grasses of both sites are C3 annual species whose growing season is during the winter to spring wet periods. Deciduous blue oaks domimate the savanna overstory of the Tonzi, with a growing season overlapping the grasses during the spring and continuing through the summer drought. In these sites, LAI measurements were available along the tower footprint for 2001 (Kiang, 2002).

Hyytiala (latitude: 61.8474150°, longitude: 24.294770°) in Finland is situated in needleleaf evergreen forest dominated by Pinus sylvestris (Scots pine), in which the phenological behavior of interest is frost-hardening. The climate is boreal. Flux measurements and soil moisture and temperature are available. For seasonal LAI, we used the site investigator's description of a constant minimum all-sided needleleaf LAI (75% of maximum) in January-May, linear increase over June to its maximum of 3.9, remaining at the maximum LAI during July-September, linear decline to its minimum in October, and a constant minimum LAI in November-December (Kolari, personal communication, 2007).

p 5835 line 12 This last sentence on PFT level parameters is out of place here, either delete it or create a new paragraph.

>> As per reviewer's suggestion, we have deleted it.

p 5835 section 5.2 This part of the discussion is somewhat general. I would be interested to see a discussion of the phenological parameters chosen and assumptions made. Is only using daylength as a senescence trigger a correct assumption? Do all sites have the same sensitivity to temperature and/or water? How sensitive are your predictions to the parameter values chosen?

>> As per reviewer's suggestion, we have added discussion about our phenology model, specifically of cold deciduous trees to tackle our assumptions about governing environment conditions for leaf onset and offset.

In the 1st paragraph of *5.2. Cold deciduousness* in the revised manuscript:
For cold deciduous trees, we used the growing degree days and chilling requirements in spring phenology (Botta et al., 2000) and temperature and photoperiod in fall phenology (White et al., 1997; Jolly et al., 2005). While we have taken a widely used approach, some

recent studies suggest other possible approaches. For spring phenology, the importance of photoperiod has been pointed out in recent studies (e.g., Korner and Basler, 2010; Migliavacca et al., 2012). Korner and Basler (2010) suggested that when the chilling requirement is fulfilled, plants become receptive to photoperiod signals and such sensitivity to photoperiod is found in late successional species in mature forests. For fall phenology, Delpierre et al. (2009) used chilling degree day-photoperiod to model leaf coloring change for deciduous trees in France, and Yang et al. (2012) and Archetti (2013) found the model suitable for New England, US, with different parameter fits. In general, despite agreement about overall climate cues for cold deciduousness, further work is needed to uncover site-independent parameterizations.

Technical comments

p 5813 line 25 "... a range of success" Rephrase.

>> This comment is not applicable, as this part does not exist in the revised manuscript.

p 5814 line 1 "This is..." This paper is?

>> We have re-written the sentence to clarify the meaning:

In this study, we perform a site-based model evaluation study for the Ent Terrestrial Biosphere Model's (Ent TBM version 1.0.1.0.0) coupled phenology/growth schemes.

p 5814 line 14 "a synthesis a variety" Delete one of your choice

>> We have corrected it to the following: *a synthesis of approaches*.

p 5823 eq. 3 Write this as e to the power of rather than exp(..)

>> We have corrected it.

p 5823 eq. 4 Equations of this type are commonly formatted as:
 This applies to equations 5-7 too.

>> We have re-written equations 5-7 as follow:

$$\varphi_T = \begin{cases} min\left(1, \frac{T_{10}-T_{min}}{T_{max}-T_{min}}, \frac{ld-ld_{min}}{ld_{max}-ld_{min}}\right) & when \ \ T_{10} < T_{max} \ \ or \ \ ld < ld_{max}, \\ 0 & otherwise. \end{cases} \quad (5)$$

$$\varphi_{SGDD} = \begin{cases} \frac{SGDD-SGDD_{crit}}{SGDD_{length}} & when \ \ SGDD > SGDD_{crit}, \\ 0 & otherwise. \end{cases} \quad (6)$$

$$\varphi_{TS} = \begin{cases} min\left(1, \frac{TS_{10}-TS_{min}}{TS_{max}-TS_{min}}\right) & when \ \ TS_{10} < TS_{max}, \\ 0 & otherwise. \end{cases} \quad (7)$$

p 5829 line 5 "the partitioning... were both larger" clumsy sentence.

>> We have re-written the sentience to clarify the meaning as follows:

However, both GPP and R_E were both more extreme in the model compared to the Fluxnet data product.

p 5834 line 28 "VPD may not a good indicator" missing "be".

>> We have corrected it.

Anonymous Referee #2

This manuscript describes the phenology module in a land surface model (Ent Terrestrial Biosphere Model, v1.0.1.0.0). The phenology module is Plant Functional Type (PFT) specific, and the authors focused on four PFTs including temperate broadleaf deciduous forest, C3 annual grassland, Mediterranean savanna, and evergreen needle-leaf forest. The authors compared the simulated timing of leaf onset and senescence with in-situ observations at four deciduous sites. The simulated and observed carbon and water fluxes are also compared.

As the author stated, this manuscript does not describe a new phenology model. Rather, the phenology module described here represents a combination of various phenology models designed for specific types of PFT. Yet, this manuscript represents an interesting and critical evaluation of the phenology model. Several critical issues (listed below) need to be address to make it a better contribution to the community.

>> We would like to express our appreciation to the reviewer for a very close, thoughtful, and helpful review.

1) One evaluation of the phenology model is the comparison between observed and simulated carbon fluxes (NEE, GPP, and Re). It should be noted that even when the phenology (i.e., start-of-season, and end-of-season) is correctly simulated, it is still possible that GPP and Re are not well quantified. The discrepancy is caused by other factors, one of which is the photosynthetic parameter Vcmax and Jmax. Description of photosynthesis and respiration is lacking in the current manuscript. Thus I recommend the authors provide a clear description of the following components:
a) Does Vcmax (and Jmax) change temporally? Field observations suggest it does (Wilson et al., Plant Cell and Envi., 2001; Bauerle et al., PNAS, 2012; Dillen et al., AFM, 2012). If Vcmax is fixed throughout the season, then it is likely causing the higher simulated GPP comparing with observation.
b) How is Vcmax determined for each site? Please provide citation to Table C1. The Vcmax of 50 umol m-2 s-1 is a bit low for Harvard Forest (see Dillen et al., AFM, 2012; Keenan et al., GCB, 2012). Yet, since Vcmax is the same vertically throughout the canopy, the overall canopy photosynthesis might be higher. Please consider using a decay function to describe Vcmax (Bonan et al., JGR-B, 2012).

>> Currently, in our model Vcmax is only variably by PFT and temperature, and the intrinsic quantum efficiency for Jmax is constant. We have been looking into how to model the seasonal variation in Vcmax mechanistically (both Vcmax and specific leaf area vary seasonally together), and also have grassland SLA data and nitrogen data in addition to the temperate broadleaf trees in the studies above mentioned. We would like to introduce the seasonal variation of Vcmax, Jmax, and SLA in a next version of our model, pending better mechanistic understanding. As the reviewer suggested, a simple approach based on photoperiod as in Bauerle et al. (2012) would be a good candidate. Thus, discussion about this issue has been added.

In the 2nd paragraph of *5.2. Photosynthesis and respiration parameters* of the revised manuscript:

Currently in the Ent model, Vcmax is only variably with PFT and temperature, and the intrinsic quantum efficiency for Jmax is constant. The seasonal variation of Vcmax, Jmax, and SLA could be introduced, pending better mechanistic understanding. A simple approach based on photoperiod such as in Bauerle et al. (2012) would be possible.

Furthermore, Vcmax has a large range of values, as well as large variation within a single site and single plant. Thus literature values for the Fluxnet sites where available were chosen, and the value within the literature range were tuned for the site. We have added the reference for Vcmax in *Appendix Table D1*.

Appendix Table D1. Biophysics parameters for Fluxnet sites in this study.

Variable	Definition	Unit	PFT4 Hyy	PFT5 Ha1	PFT6 MMS	PFT7 Ton (oak)	PFT13 Var & Ton (grass)
P_{st}	Pst - photosynthetic pathway	-	C3	C3	C3	C3	C3
PAR_{absorb}	Leaf PAR absorbance	-	0.93	0.90	0.90	0.90	0.86
V_{cmax} [1]	Maximum photosynthetic capacity	$\mu mol\ m^{-2}\ s^{-1}$	43.0^2	60.0^2	51.0^3	56.4^4	50.1^4
m	Slope of Ball-Berry stomatal conductance equations	-	9.0	9.0	9.0	9.0	11.0
b	Intercept of Ball-Berry stomatal conductance equation	$\mu mol\ m^{-2}\ s^{-1}$	0.002	0.002	0.002	0.002	0.008

[1]*For all these plant functional types there is a large range of values, as well as large variation within a single site and single plant. We therefore have chosen literature values for the Fluxnet sites where available, and tuned the value within the literature range for the site.*
[2]*Oleson et al. (2004)*
[3]*Wilson et al. (2001)*
[4]*Wang et al. (2007)*

2) A clear description of the data is lacking. I suggest that the authors provide a section solely for this purpose.
For example, LAI observations are used for validation at a couple of sites. How was LAI measured? If LAI was measured manually using LAI-2000, what was the temporal frequency? How were 20%, 50%, and 80% dates of observed LAI determined? Have you used any function to fit the data?
Eddy covariance data were used in the work. Thus it is necessary to briefly describe this dataset, including the temporal frequency and the separation method between the GPP and respiration (citations are needed).

>> To describe the site data, we have written a separate subsection of 3.1. Fluxnet sites.

In *3.1. Fluxnet sties* of the revised manuscript:
    The Ent TBM was evaluated at five Fluxnet sites, including Morgan Monroe State Forest, Harvard Forest, the Vaira Ranch, the Tonzi Ranch and Hyytiala, as briefly mentioned above (Table 3). From all sites, data from the flux tower systems were available. Meteorological driver data include radiation, precipitation, air temperature, air pressure, humidity and wind, used to drive the model. Soil moisture and temperature measurements were also used to drive the Ent standalone simulations. Flux data includes net ecosystem

exchange (NEE) and evapotranspiration (ET), and were used to evaluate the simulation results. Among sites, data availability, such as LAI, varied and suited different types of model simulations as described in detail in the next section.

The Morgan Monroe Sate Forest (MMSF), located in Indiana, USA (Schmid et al., 2000) (latitude: 39.32315°, longitude: -86.413139°) is is an extensive managed temperate broadleaf deciduous forest with a total area of 95.3 km2. The area is covered primarily by a secondary successional broadleaf forest within the maple-beech to oak-hickory transition zone of the eastern deciduous forest, dominated by supar maple and tuilip poplar. LAI measurements at 5-14 day intervals during the growing season were available for 1998-2001 {Andrew Oliphant, 2006 #1646}).

Harvard Forest (latitude: 42.5313°, longitude: -72.1898°) is an eastern temperate mixed forest dominated by deciduous trees. The area surrounding the flux tower is dominated by red oak and red maple, with scattered stands of Eastern hemlock, white pine and red pine. About 1/3 of the existing red oaks were established prior to 1895, another 1/3 prior to 1930, and the rest before 1940, and thus the stand is 75–110 years old (Urbanski et al., 2007). O'Keefe (2000) provides the leaf phenology of Harvard Forest. The timings of spring leaf development and fall leaf fall have been recorded for permanently tagged individuals in the field from 1991. The leaf development and senescence data in percent of final leaf size have been used to obtain 'observational' LAI based on the maximum LAI in the model, i.e., (observed LAI) = (observed % of leaf development or fall) X (modeled maxmimum LAI).

The Vaira Ranch (latitude: 38.4066667°, longitude: -120.950733°) and Tonzi Ranch (latitude: 38.4316°, longitude: -120.9660°) in Ione, California, are located in an open grassland ecosystem and an oak/grass savanna ecosystem, respectively, in a Mediterranean climate of cool wet winters, and dry hot summers. The sites are less than 3 km apart. The grasses of both sites are C3 annual species whose growing season is during the winter to spring wet periods. Deciduous blue oaks domimate the savanna overstory of the Tonzi, with a growing season overlapping the grasses during the spring and continuing through the summer drought. In these sites, LAI measurements were available along the tower footprint for 2001 in approximately 2-week increments during the growing season (Kiang, 2002).

Hyytiala (latitude: 61.8474150°, longitude: 24.294770°) in Finland is situated in needleleaf evergreen forest dominated by Pinus sylvestris (Scots pine), in which the phenological behavior of interest is frost-hardening. The climate is boreal. Flux measurements and soil moisture and temperature are available. For seasonal LAI, we used the site investigator's description of a constant minimum all-sided needleleaf LAI (75% of maximum) in January-May, linear increase over June to its maximum of 3.9, remaining at the maximum LAI during July-September, linear decline to its minimum in October, and a constant minimum LAI in November-December (Kolari, personal communication, 2007).

3) Just food for thought on the phenology model for temperate deciduous forests. It has been recognized that for sites like Harvard Forest, the chilling requirements are always fulfilled, and photoperiod plays an important role in controlling the start of heat accumulation. Models with an explicit chilling requirement do not perform better than those without chilling requirements (see Migliavacca et al., Biogeosciences, 2008; Yang et al., JGR-B, 2012; Korner and Basler, Science, 2010). And the first two papers that used Harvard Forest as the study site suggest a temperature+photoperiod model is a better choice. I suggest that the authors consider other forms of phenology models, especially those with photoperiod controls – the dominant deciduous species at Harvard Forest include oak and maple are likely controlled by

temperature and photoperiod (Korner and Basler, 2010). Even if a full comparison is not possible, a paragraph in discussion on the controls of spring phenology in temperate deciduous forests is necessary.

>> The suggested references point out the importance of photoperiod for spring phenology, but it is also implied that such sensitivity to photoperiod is not universal to all cold deciduous trees (Korner and Basler, 2010). We therefore have added such discussions with the suggested references.

In the 1ˢᵗ paragraph of *5.2. Cold deciduousness* in the revised manuscript:
For cold deciduous trees, we used the growing degree days and chilling requirements in spring phenology (Botta et al., 2000) and temperature and photoperiod in fall phenology (White et al., 1997; Jolly et al., 2005). While we have taken a widely used approach, some recent studies suggest other possible approaches. For spring phenology, the importance of photoperiod has been pointed out in recent studies (e.g., Korner and Basler, 2010; Migliavacca et al., 2012). Korner and Basler (2010) suggested that when the chiling requirement is fulfilled, plants become receptive to photoperiod signals and such sensitivity to photoperiod is found in late sucessional species in mature forests. For fall phenology, Delpierre et al. (2009) used chilling degree day-photoperiod to model leaf coloring change for deciduous trees in France, and Yang et al. (2012) and Archetti (2013) found the model suitable for New England, USA, with different parameter fits. In general, despite agreement about overall climate cues for cold deciduousness, further work is needed to uncover site-independent parameterizations.

4) The fall phenology model for temperate deciduous forests produces results 30-50 days biased from the observation (Fig.3). This is not entirely an unreasonable result, as we know that fall phenology is even harder to model comparing with the spring phenology. However, recent advances in modeling fall phenology do show some promising results (see Delpierre et al., AFM, 2009; Archetti et al., Plos ONE, 2013). I suggest that the authors test these fall phenology models (using optimized parameters from these papers).

>> For fall phenology of cold deciduous tree, we have used the temperature and photoperiod as in Eq. 5 with modifications to White et al. (1997) and Jolly et al. (2005) as their approaches have been evaluated for US and the globe, respectively. On the other hand, Archetti et al. (2013), modified from Delpierre et al. (2009), used the same variables but with different functional forms and evaluated the model for a New England Forest. We agree that it would be interesting to evaluate Archetti et al.'s model, and thus we have added the suggested references in the text to note them as a possible approach could be utilized in the future.

In the 1ˢᵗ paragraph of *5.2. Cold deciduousness* in the revised manuscript:
For cold deciduous trees, we used the growing degree days and chilling requirements in spring phenology (Botta et al., 2000) and temperature and photoperiod in fall phenology (White et al., 1997; Jolly et al., 2005). While we have taken a widely used approach, some recent studies suggest other possible approaches. For spring phenology, the importance of photoperiod has been pointed out in recent studies (e.g., Korner and Basler, 2010; Migliavacca et al., 2012). Korner and Basler (2010) suggested that when the chiling requirement is fulfilled, plants become receptive to photoperiod signals and such sensitivity to

photoperiod is found in late sucessional species in mature forests. For fall phenology, Delpierre et al. (2009) used chilling degree day-photoperiod to model leaf coloring change for deciduous trees in France, and Yang et al. (2012) and Archetti (2013) found the model suitable for New England, USA, with different parameter fits. In general, despite agreement about overall climate cues for cold deciduousness, further work is needed to uncover site-independent parameterizations.

Specific comments (P for page, L for line):

P5810 L23: do you mean "a major weakness in DGVMs"? This sentence is not well structured and lacks connection with the next sentence. Please consider revising it.

Please be advised that a mistake in the copyediting process led the incomplete sentence in the beginning of the manuscript. We have corrected it.

In the 1st paragraph of *1. Introduction* of the revised manuscript:
Phenological timing remains a major weakness of land surface dynamic global vegetation models (DGVMs) that are coupled to general circulation models (GCMs), and a primary cause of uncertainty in predicting the trajectory of global atmospheric CO2 (Friedlingstein et al. 2006, Friedlingstein et al. 2014).

P5820 L14: "ntropical" to "tropical". >> We have corrected it.

P5822 L21: The correct form of eq (1) should have the sum of max(0,T10-Tbase), not the other way around. In addition, please state the date from which the heat accumulation (and chilling day accumulation) starts. Please be specific about "the beginning of the winter season".

>> We have corrected the equation as follows:
$$GDD = \sum \max(0, T_{10} - T_{base}).$$
(1)
Also, the phrase was clarified as follows:
at the beginning of the winter season (when Phenostatuscd switches from 4 to 1).

P5823 L16: What control the rate of leaf dropping? P5831 L14: Please add the unit for the "RMSE of ~0.4"

>> We have added unit as follow: *RMSE of ~0.4 μmol/m2/s.*

P5833 L5: Where is Fig.9? Did you mean "Fig. 8"? Please also provide evidence that " a relatively small difference in ET was detected between the simulations with and without the frost-hardening scheme".

>> We have corrected it to Fig. 8. As well, we have clarified the sentence with the evidence.

In the 1st paragraph of *4.3.2. Fluxes* of the revised manuscript:
Frost-hardening suppressed photosynthetic capacity during the winter (particularly in Feb-April) and therefore GPP and NEP. It also suppressed transpiration and thus ET, but a

relatively small difference in ET was detected between the simulations with and without the frost-hardening scheme as the RMSEs with observations were 7.88 mm/s and 7.89 mm/s, respectively (Table 6).

P5837 L10: Results from this manuscript do not provide evidence to the statement starting from "we found that the ED scheme . . .". Please provide additional evidence (or references).

>> The ED scheme impacts our simulated carbon fluxes, although not the phenology, so we wished to mention this for future work. We did not think a plot of sapwood variation as necessary for this paper, because it was not realistic, is not a widely used scheme, and would not have lent insight to the literature. As per reviewer's suggestion, we have re-written the paragraph as follows:

Although the ED carbon allocation/growth scheme is not the topic of this study, it is necessary to address how deficiences we encountered in this scheme impacted our carbon flux results. Although the current carbon allocation and growth scheme results in LAI that is reasonable, with some phenological timing issues as noted, the maximum LAI is achieved thanks to a cap on LAI by allometric relations to stem structure and plant density, while the rest of the plant carbon balance is not realistic, particularly with regard to rate of LAI growth, amount of seasonal sapwood growth and conversion to heartwood, accumulation of carbon reserves, and allocation to reproduction. The on/off cues of the Ent phenological factor for cold deciduous trees results in unrealistic fast full leaf-out, which could be rectified by introduction of a physically-based cell growth elongation factor (Lockhart 1965). For future work, we determined it would be more realistic to make carbon allocation to each live pool independent. The ED scheme's allocation to one live biomass total and then partitioning among the live pools can lead to unrealistic behaviors for sapwood patterns during spring growth and fall senescence, due to a partitioning scheme for live carbon that does not account for the different seasonal behaviors of each live pool.

Figure 3: This figure does not show how the simulated LAI compare with observation in terms of the absolute value of LAI. It will be great to see the seasonal patterns of LAI, for which if the absolute value is not simulated correctly might have a profound effect on the magnitude of GPP.

>> In this study, we use an "active biomass" phenology-only mode: canopy stem structure is prescribed and static, while seasonal leaf and fine root dynamics are prognostic. Therefore the annual maximum of LAI was fixed in the model as observed. We therefore simply presented the LAI relative to it annual maximum.

Variability of phenology and fluxes of water and carbon with observed and simulated soil moisture in the Ent Terrestrial Biosphere Model (Ent TBM version 1.0.1.0.0)

Y. Kim[1,2], P. R. Moorcroft[3], I. Aleinov[4], M. J. Puma[4], N. Y. Kiang[2]

[1]{Department of Civil and Environmental Engineering, Yonsei University, Seoul 120-749, Korea}

[2]{NASA Goddard Institute for Space Studies, New York, NY 10025, USA}

[3]{Department of Organismic and Evolutionary Biology, Harvard University, Cambridge, MA 02138, USA}

[4]{Center for Climate Systems Research, Columbia University, New York, NY 10025, USA}

Correspondence to: Yeonjoo Kim (yeonjoo.kim@yonsei.ac.kr)

Abstract

The Ent Terrestrial Biosphere Model (Ent TBM) is a mixed-canopy dynamic global vegetation model developed specifically for coupling with land surface hydrology and general circulation models (GCMs). This study describes the leaf phenology submodel implemented in the Ent TBM version 1.0.1.0.0, coupled to the carbon allocation scheme of the Ecosystem Demography (ED) model. The phenology submodel adopts a combination of responses to temperature (growing degree days and frost-hardening), soil moisture (linearity of stress with relative saturation), and radiation (light length). Growth of leaves, sapwood, fine roots, stem wood, and coarse roots is updated on a daily basis. We evaluate the performance in reproducing observed leaf seasonal growth as well as water and carbon fluxes for four plant functional types at five Fluxnet sites, with both observed and prognostic hydrology, and observed and prognostic seasonal leaf area index. The phenology submodel is able to capture the timing and magnitude of leafout and senescence for temperate broadleaf deciduous forest (Harvard Forest and Morgan-Monroe State Forest, US), C3 annual grassland (Vaira Ranch,

1

US), and California oak savanna (Tonzi Ranch, US). For evergreen needleleaf forest (Hyytiäla, Finland), the phenology submodel captures the effect of frost-hardening of photosynthetic capacity on seasonal fluxes and leaf area. We address the importance of customizing parameter sets of vegetation soil moisture stress response to the particular land surface hydrology scheme. We identify model deficiencies that reveal important dynamics and parameter needs.

1 Introduction

Phenological timing remains a major weakness of land surface dynamic global vegetation models (DGVMs) that are coupled to general circulation models (GCMs), and a primary cause of uncertainty in predicting the trajectory of global atmospheric CO_2 (Friedlingstein et al. 2006, Friedlingstein et al. 2014). Seasonal variation of vegetation foliage, i.e., leaf phenology, determines the timing and duration of the photosynthetically active canopy, influencing stomatal activity, surface albedo and surface roughness (Jolly and Running 2004). Thus, it plays a crucial role in the exchange of water, energy and carbon between land and the overlying atmosphere. Numerous observations show that the interannual variability of transpiration and gross primary productivity is associated with timings of leaf-out and leaf senescence across ecosystem types (Goulden et al., 1996). Light-controlled leaf phenology is suggested as a key controlling factor responsible for increasing carbon and water fluxes from land to the atmosphere during the dry season in the Amazon rainforests (Hutyra et al. 2007, Kim et al. 2012). Phenology is also tightly connected to other ecosystem processes, exerting strong controls on the amount of assimilated carbon that is subsequently utilized for plant growth and reproduction. Kramer (2000) showed that phenology could have effects on the species composition of temperate-zone deciduous forests and the geographical distribution of species since difference in phenological response leads to difference in light availability and therefore growth in mixed species stands. Given the strong interactions between phenology and other land surface and ecosystem processes, phenology affects both weather and climate. Seasonal variation in vegetation characteristics have been shown to significantly influence summer precipitation and temperature in the U.S. (Dirmeyer 1994, Xue et al. 1996), and enhance or weaken the feedbacks between soil moisture and precipitation in the continental interior of North America depending on soil moisture conditions and season (Kim and Wang 2007). Levis and Bonan (2004) demonstrated that the coupling between phenology and the

2

atmosphere is critical for models to capture seasonal weather evolution. Tightly linked to phenology, plant carbon allocation, that is, distribution of assimilated carbon among the plant parts, also responds to environmental and climate conditions (such as increases in air temperature, changes in precipitation patterns and elevated atmospheric CO_2 concentration). For example, Pumpanen et al. (2012) observed that root biomass and the rate of photosynthesis for silver birch, Norway spruce and Scots pine seedlings increase with higher soil temperature, yet a simultaneous increase in both photosynthesis and respiration rates results in no change in net CO_2 exchange and total seedling biomass.

Terrestrial biosphere models (TBMs) or Dynamic Global Vegetation Models (DGVMs) have been developed and coupled to General Circulation Models (GCMs) (e.g., Foley et al. 1996, Cox 2001, Sitch et al. 2003, Bonan and Levis 2006, Dunne et al. 2013), to account for biophysical and biogeochemical processes and sometimes biogeography, allowing prediction of transient terrestrial ecosystem interactions with climate (Cramer et al. 2001, Friedlingstein et al. 2006). Thus the active role of vegetation phenology can be incorporated into climate modeling. TBMs have been parameterized and evaluated on the basis of local, regional, or global scale studies. It has become common to evaluate the models at the individual field scale at sites with eddy flux measurements and detailed ground data (e.g., Delire and Foley 1999, Arora and Boer 2005, Krinner et al. 2005, Kucharik et al. 2006, Friend et al. 2007, Stöckli et al. 2008, Bonan et al. 2011). Still, parameterizations for vegetation processes (such as phenology and carbon allocation) implemented in TBMs are often limited to local-scale derivations due to the lack of high-quality global scale observations of vegetation structure and function together with meteorological conditions and mechanistic understanding free of local effects.

Prognostic phenology models have been developed to predict phenological response of vegetation to climate based on empirical evidence, as a mechanistic, process-based treatment is still not fully realizable wtih current understanding (Sala et al. 2012). The more commonly used climatic rule-based approach accounts for cues by temperature, soil moisture, and day length cues to phenology, to predict leaf-on and leaf-off, with these controls often represented as a cumulative functions of one or several climate variables that reach an empirically defined threshold (White et al. 1997). Another approach is based on plant carbon status (Bonan et al. 2003), and predicts leaf-out and senescence on the basis of potential

3

positive carbon assimilation, which is in turn is affected by temperature, moisture, and sometimes nutrient conditions.

All of the above approaches require empirical parameterization of the responses to climate, and a model scheme that is independent of PFT or geographical variation is still a research goal. Jolly et al. (2005) have proposed a very simple and promising bioclimatic Growing Season Index (GSI) for phenology based on linear relations to minimum temperature, photoperiod, and vapor pressure deficit (VPD, as a proxy for soil moisture), which seems to perform well compared to satellite observations at diverse sites. However, it performs less well for arid systems for which VPD may not be a good indicator of available deep soil moisture, and it is not able to capture any seasonal moisture or light sensitivity that has been observed in tropical evergreen forests (Stockli et al. 2011). Forkel et al. (2014) adopted the concept of GSI but used the soil water availability instead of VPD for water limiting function. Phenology depends not only on atmospheric water demand but also on water supply from soil moisture as Migliavacca et al. (2011) have shown that GSI performed better when using a soil moisture limiting function instead of the VPD limiting function. Recently, Caldararu et al. (2014) introduced a promising optimality approach based on the hypothesis that phenology is a strategy for optimal leaf area index, rather than explicit carbon exchange, driven by canopy-level demand for – and constrained by availability of -- light and water, limited by leaf aging. They fitted the model to satellite observations of LAI and demonstrated its capability to reproduce phenological patterns for different vegetation types over the globe within 8-16 days of observations. Top-down optimality approaches such as this may indeed be the smart way for global scale models way to capture the strategic behaviors inherent in phenology in lieu of mechanistic understanding at the leaf or molecular level; the next step remains to couple them with explicit carbon exchange and allocation.

In this study, we perform a site-based model evaluation study for the Ent[1] Terrestrial Biosphere Model's (Ent TBM version 1.0.1.0.0[2]) coupled phenology/growth schemes. This

---

[1] Ent is not an acronym but the name of a sentient species of tree in J.R.R. Tolkien's fantasy novels, The Lord of the Rings.
[2] Enumeration is in order for different levels of dynamics and different physics versions available for each of these. In order, the digits denote:
1) Primary biophysics (leaf, soil biogeochemistry) and base release version (1: leaf biophysics as described in Schmidt et al. 2014; soil biogeochemistry described in this paper).
2) Canopy radiative transfer (0: two-stream as described in Schmidt et al. 2014; 1: ACTS

4

evaluation is a necessary task before introducing prognostic phenology into global simulations coupled with a GCM atmosphere in order to enable modeling of interactive phenology and climate. We do not offer yet a new paradigm, but the phenological timing schemes provide a synthesis of approaches in the literature to capture the full combination of climatological drivers thus far known to be essential for each type of phenology, and introduce some new functional representations to do so. These are coupled to growth algorithms from the Ecosystem Demography (ED) model (Moorcroft et al. 2001) that account for both the geometric and mass allometry of plant functional types.

In this paper, we describe the Ent TBM's phenology and allometry scheme coupled to the ED carbon allocation scheme, and evaluate their performance at Fluxnet sites (Baldocchi et al. 2001), focusing on seasonal and inter-annual variations of LAI and carbon and water fluxes. We compare site simulations using both observed soil moisture and that modeled by a land surface hydrology model coupled to the Ent TBM. The phenology schemes synthesize several observational data sets, combining both climate responses and a carbon balance approach, described in detail below. Here we evaluate the performance for temperate broadleaf deciduous forest, C3 annual grassland, evergreen needleleaf forest, and tree/grass savanna (mixed drought deciduous broadleaf and C3 annual grassland). Through these evaluations, we are interested in quantifying the accuracy of the current model at the site level, and we identify ecosystem processes needing further improvement, with regard to both plant growth dynamics and the representation of soil moisture.

2   Model descriptions

2.1   Land Surface Model (LSM) of the NASA GISS GCM

The Ent TBM can be run with observed soil moisture and temperature, and canopy temperature inferred from eddy flux measurements of sensible heat fluxes, or, given precipitation and air temperature, it can obtain modeled soil moisture, temperature, and

---

model (Ni-Meister et al. 2010; Yang et al., 2010);
3) Leaf phenology (0: prescribed from satellite data; 1: prognostic, this paper);
4) Carbon allocation/growth (0: allocation with prognostic phenology, without structural growth, this paper; 1: allocation with structural growth).
5) Ecosystem dynamics (0: none; 1: Ecosystem Demography scheme).

5

1 canopy temperature, if run coupled to a land surface hydrology model. For the coupled mode,

2 we use the land model of the National Aeronautics and Space Administration (NASA)

3 Goddard Institute for Space Studies (GISS) general circulation model (GCM) (Schmidt et al.

4 2006). The NASA GISS GCM land hydrology consists of six soil layers down to 3.5 m depth

5 based on Rosenweig and Abramopoulos (1997), with updates described in Schmidt et al.

6 (2006; 2014). The land surface model (LSM) computes the fluxes of heat and water vapor to

7 the atmosphere, and the energy balance of the soil and vegetation canopy. Surface runoff is

8 calculated based on saturation and infiltration capacity of the upper soil layer. The

9 underground runoff is computed according to a formulation of Abramopoulos et al. (1988),

10 which takes into account the average slope and the density of underground sinks in the cell.

11 When running the Ent TBM coupled to the GISS LSM, soil physics parameters are taken

12 from the land surface mapped datasets of the GISS LSM.

13 **2.2 Ent Terrestrial Biosphere Model (Ent TBM)**

14 The Ent TBM is a standalone model developed specifically for coupling the fluxes of water,

15 energy, carbon, and other trace gases between LSMs and GCMs. It is structured like the ED

16 model (Moorcroft et al. 2001) for simulating competition in mixed canopies and disturbance

17 dynamics by representing vertical canopy structure through ensemble cohorts of identical

18 individuals, and horizontal heterogeneity via subgrid patch communities. The specifications

19 of canopy geometry and allometry of biomass pools are consistent with indvidual ellipsoidal

20 crown geometry that is integrated with the coupled phenology/growth model. This paper

21 presents simulations of seasonal variation in leaf area and mass and in fluxes of CO_2, water

22 vapor, and sensible and latent heat of both transpiration and ground evaporation.

23 Fig. 1 shows a conceptual diagram of the Ent model, and how it is coupled with a GCM (or

24 off-line meteorological forcings) and an LSM. Ent's biophysics modules operate at the

25 physical time step of the GCM or LSM. The photosynthetic uptake of carbon utilizes the

26 well-known photosynthesis model of Farquhar et al. (1980) and Farquhar and von Caemmerer

27 (1982) coupled with the stomatal conductance model of Ball and Berry (Ball et al. 1987),

28 while Ent uses its own cubic solution for these coupled equations. Canopy radiative transfer

29 is optionally modeled as in Friend and Kiang (2006) for homogeneous canopies, or as in Ni-

30 Meister et al. (2010) and Yang et al. (2010) for clumped canopies. In this paper, in lieu of

31 detailed site allometric and canopy structure data, we utilize the homogeneous canopy

32 radiative transfer scheme. Carbon uptake is accumulated over a day so that carbon allocation

6

to growth, phenological behavior, and mortality are updated once per day. An individual plant has distinct biomass pools, including a "labile" or carbohydrate reserve pool into which photosynthetic uptake and retranslocated carbon are accumulated; "active" pools consisting of foliage, fine roots, a reproductive pool, and, for woody plants, live sapwood, and "dead" pools consisting of dead stem wood and coarse roots. Autotrophic respiration is the sum of maintenance respiration as function of biomass and temperature, "activity growth respiration" as function of gross assimilation, and tissue growth respiration as a function of amount of new growth.

Ent takes its meteorological drivers and hydrological balance at the grid cell or catchment zone scale of the LSM and subgrid heterogeneity is represented as dynamic patches of vegetation communities, comprised of cohorts of plants that are ensembles of identical individuals (patch and community dynamics are not part of this study). The biomass pools and geometry of an individual woody plant are illustrated in Fig. 2 Canopy conductances from each patch are summed to the grid cell or catchment zone level to couple with the atmosphere. Also, root density vertical profile distributions in Ent are used to calculate a depth-weighted average of soil moisture stress. These profiles are a modification of those in Rosenzweig and Abramopoulos (1997), with details given in the Appendix A.

The Ent TBM is designed to support a flexible number of plant functional types (PFTs). A parameter set for 17 PFTs has been developed, as listed in Table 1; however, we note that only a subset of these PFTs is evaluated here according to data availability, and the others must be approximated from the available similar types and theoretical/empirical relations from the literature. Following the rationale first advocated by Defries et al.(1995) and adopted by all vegetation models since then to varying degrees, Ent's PFTs distinguish photosynthetic pathway (C3 and C4), phenological type (evergreen, cold deciduous and drought deciduous), leaf type (broadleaf and needleleaf), growth form (tree, shrub, and herbaceous), and cultivated (herb crops). In addition, to better capture community dynamics in mixed canopies, if parameter sets are provided, Ent has the capability to distinguish early and late successional species through differences in leaf life span, following the approach of the ED model (Moorcroft et al. 2001), which is based on leaf physiological relations found in Reich et al. (2007).

To capture total net carbon fluxes, the Ent TBM incorporates the code implementation of CASA' from the Community Land Model 3.0 (CLM 3.0, Randerson et al. 2009; Doney et al.,

7

2006; code kindly supplied by Jasmin John), which is based on the Carnegie-Ames-Stanford-Approach of Potter et al. (1993). For the Ent TBM, the CASA' temperature and soil moisture responses of respiration were replaced with functions derived from new fits to field data of Del Grosso et al. (2005). Details are provided in Appendix B.

As mentioned earlier, the Ent TBM can be run in several different modes of coupling: (1) a stand-alone mode when the meteorological (e.g., radiation, precipitation, air temperature, air pressure, humidity and wind) and land conditions (e.g., soil moisture and soil temperature, and canopy temperature) are provided ("Ent-standalone"), (2) a mode coupled with a LSM for prognostic soil moisture and temperature given meteorological forcings ("Ent-LSM"), and (3) a fully coupled mode with an atmospheric GCM. Ent-standalone and Ent-LSM modes can be used for site-specific simulations or regional/global simulations using observed meteorological and soil moisture data.

The Ent TBM can also be run with different levels of vegetation dynamics turned on or off. In a biophysics-only mode, canopy structure and leaf area are prescribed, to simulate only fluxes of water vapor, carbon dioxide, and other trace gases. In an "active biomass" phenology-only mode, canopy stem structure is prescribed and static, while seasonal leaf and fine root dynamics are prognostic, and carbon that would have been allocated to stem and coarse root growth instead is allocated to litter. In a phenology-woody growth mode, in addition to leaf phenology, stem and coarse root growth are also enabled. In an ecosystem-dynamics mode, mortality and disturbance ensure that plants cannot grow indefinitely and are subject to succession and cover change (ecosystem dynamics are not covered in this paper).

2.3 Plant growth submodel

The plant growth submodel integrates phenological timing and allocation of carbon to growth and litter fluxes (background litterfall and seasonal), and respiration fluxes tied to tissue growth. The phenology scheme determines the phenological status of plants based on various environmental and climate rules studies, which determine budburst, frost-hardening, and senescence according to the phenological types of plants such as drought-deciduousness and cold-deciduousness. The carbon fixed over the course of each day from photosynthesis is accumulated and placed into a labile carbohydrate reserve pool. Carbon from the labile pool is then allocated once per day into different plant pools of foliage, sapwood, heartwood, fine root and coarse root as well as a reproductive pool according to empirical allometric

8

1 relationships and leaf phenological status. In addition, tissue lost to background litter fluxes

2 is replenished, and respiration fluxes are produced from growth of any tissue. A portion of

3 litterfall is retranslocated back to the labile pool.

4 In the Ent TBM, the carbon allocation scheme takes a traditional approach of 'static

5 allocation', based on fixed allometric relationships between different pools. Adopted from

6 approaches of the ED models (Moorcroft et al. 2001, Medvigy et al. 2009). Appendix C

7 provides the descriptions of the ED allocation scheme, which treats "active" and "dead"

8 biomass pools as bulk sinks, with modifications for Ent. We identified some deficiencies of

9 the ED allocation scheme, and suggest future work for improvement in Section 5. Also note

10 that Appendix D provides the biophysical, phenological and allocation parameter values used

11 in this study.

12 Full prognostic growth entails growth of woody structure and the size of woody plants, which

13 would require in addition full mortality and establishment dynamics so that there is not

14 unlimited growth; these population and community dynamics will be presented in future

15 papers. This study focuses on the "active biomass" performance of Ent given seasonal

16 phenology, keeping woody structure static, allocating the amount that would have gone to

17 growth instead to litterfall.

2.4 Phenology

19 The phenology scheme in the Ent TBM provides a synthesis, and combines the climatic rule-

20 based approach and carbon balance for deciduous plants to determine the timings and rates of

21 leaf out and leaf senescence by integrating several different modeling studies. We present a

22 diversity of PFTs, adding those with known behaviors that depart from common

23 representations of cold, drought, or light responses. While globally applicable

24 parameterizations of climate rule-based phenology may still be elusive, where available in the

25 literature, we draw from wide surveys that attempt to extrapolate to the global scale.

26 For deciduous plants, we use parameterizations by Botta et al. (2000). With growing degree

27 day (GDD) and chilling requirement, they examined the possibility of extrapolating existing

28 local models for leaf onset date to the global scale by retrieving leaf onset dates from the

29 NOAA/AVHRR satellite normalized difference vegetation index (NDVI). They identified

30 appropriate leaf onset date models and estimated their parameters for each biome, which are

31 implemented in other ecosystem models (Medvigy et al. 2008). The importance of a chilling

9

requirement is confirmed by Richardson et al. (2012), who conducted an inter-comparison of phenology predictions of eleven TBMs (and three biophysics models with prescribed phenology) at five deciduous broadleaf and five evergreen needleleaf Fluxnet sites. They found that, for deciduous forests, the models consistently predicted an earlier onset of the growing season and later fall senescence than observed; meanwhile, most models under-predicted the magnitude of peak GDD sums, while those that explicitly or implicitly included a chilling requirement did relatively well in capturing the onset of LAI and GPP for deciduous and evergreen forests, compared to simple temperature threshold schemes. For drought deciduous trees and grasses, we also make use of parameterizations of White et al. (1997) who developed a regional phenology model for the US, predicting timings of leaf onset and offset based on the satellite NDVI at the 20 km resolution. Their prediction errors are ~1 week, and maximum expected errors are 10-14 days.

For evergreen vegetation, the Ent TBM includes frost-hardening for boreal evergreen plants. The frost-hardening (also called winter cold-hardening) involves physiological changes to protect the plant from chilling injury and freezing injury, leading to a downgrading of leaf photosynthetic capacity as well as tissue turnover and respiration. Coniferous vegetation in the boreal zone has a clear annual cycle of photosynthetic activity, with photosynthesis low or zero during the winter, increasing during the spring, peaking during the summer, and decreasing during the fall. While part of the cycle is due to direct responses to PAR and air temperature, the inherent photosynthetic capacity of needles also changes (Makela et al. 2004). Therefore, the models that do not account for cold-hardening and de-hardening will over-predict the uptake of carbon by photosynthesis for boreal systems during the late fall through early spring. This study implements a frost-hardening algorithm based on Hanninen and Kramer (2007), Makela et al. (2006) and Repo et al. (1990), who developed a model of the frost-hardiness of the stems of Scots pine seedlings. Below we describe the explicit model functions reflecting our choices based on the literature above.

2.4.1 Phenology Model Climate Cue Framework

In the Ent TBM, several "phenological factors", φ_x, as well as physiological stress factors, β_x, are calculated for seasonal environmental cues from various climate measures x. These include air and soil temperature history (cumulative number of growing degree days and of

10

chilling days), day-length and soil moisture. The phenological factors control the allocation of assimilated carbon, while the physiological stress factors affect the efficiency of carbon uptake, and all range from 0 to 1 on a daily basis. Different rules apply to the different PFTs, according to phenotype (woody plant cold-deciduous, cd; drought-deciduous, dd, evergreen, ev; tropical radiation phenology, tr; and cold deciduous herbs, c, whether annual or perennial). The phenological factor controls the timing and rate of carbon transfer between the labile and active carbon pools and hence the seasonal variation in leaf area index (LAI), fine roots, and sapwood.

Furthermore, the Ent TBM determines "phenological status", $Phenostatus_p$, where p is the phenotype, which identifies phenologically different seasons. For plants with seasonal leaf-out and senescence, $Phenostatus_p$ is 1 for the leaf-off season, 2 for the leaf-up period, 3 for the peak foliage period, and 4 for the senescent period. The trend in length of day (ld) is used to determine which season it is, or, rather, which half of the year it is. If day length is decreasing, then it is the latter half of the year, and "fall" may be allowed to commence, depending on other climate variables of phenological factors. Below we itemize these variables and equations in the Ent phenology scheme.

2.4.2 Cold deciduous woody plants

During the winter, the phenological status of cold-deciduous trees and shrubs, $Phenostatus_{cd}$, is 1, for no foliage. Leaf-out ($Phenostatus_{cd}=2$) occurs once the cumulative number of growing degree days (GDD) exceeds its critical number (GDD_{crit}), which is determined with a function of cumulative number of chilling days (NCD) (Botta et al. 2000). Following Kim and Wang (2005), the 10-day running average of air temperature (T_{10}) difference from the base temperature (T_{base}) of 5°C is used to calculate GDD and NCD on a daily basis as follows:

$$GDD(t) = GDD(t-1) + \max(0, T_{10} - T_{base}) \tag{1}$$

$$NCD(t) = NCD(t-1) + 1 \quad if \quad T_{10} < T_{base}. \tag{2}$$

where t is time in days. GDD and NCD are reset to be zero at the beginning of the winter season (when $Phenostatus_{cd}$ switches from 4 to 1). The function for GDD_{crit} is expressed as follows:

$$GDD_{crit} = GDD_{intercept} + GCC_{slope} e^{(NCD_{multi} \cdot NCD)} \tag{3}$$

where the constant values of $GDD_{intercept}$, GDD_{slope} and NCD_{multi} are provided in Table 2.

11

Once leaf-out starts, trees take a number of degree days (GDD_{length}) to reach the phenologically unconstrained status (Foley et al. 1996). We introduce an approach to scale the departure of GDD from GDD_{crit} with GDD_{length}, and to have a phenology factor, φ_{GDD}, that ranges from 0 to 1:

$$\varphi_{GDD} = \begin{cases} \dfrac{GDD-GDD_{crit}}{GDD_{length}} & \text{when } \ GDD > GDD_{crit}, \\ 0 & \text{otherwise.} \end{cases} \quad (4)$$

When $\varphi_{GDD}=1$, then the *Phenostatus*$_{cd}$ switches to 3, peak foliage. Full or peak foliage may also occur when carbon allocation to foliage reaches the maximum supported by the available sapwood.

Fall senescence (*Phenostatus*$_{cd}$=4) can commence in response to shortening day length ("fall") and decreased air temperature, in a modification of White et al. (1997) and Jolly et al. (2005). Leaves start dropping once air temperature or day length decreases down to threshold values (i.e., T_{max} and ld_{max}) proportionally to the temperature decreases in the fall as in Eq. (5). Full senescence finally occurs when air temperature or day length decrease further down to the minimum thresholds (i.e., T_{min} and ld_{min}). The phenological factor with respect to air temperature, φ_T, is:

$$\varphi_T = \begin{cases} \min\left(1, \dfrac{T_{10}-T_{min}}{T_{max}-T_{min}}, \dfrac{ld-ld_{min}}{ld_{max}-ld_{min}}\right) & \text{when } \ T_{10} < T_{max} \ \text{ or } \ ld < ld_{max}, \\ 0 & \text{otherwise.} \end{cases} \quad (5)$$

T_{max}, T_{min}, ld_{max} and ld_{min} are constants, with values provided with references in Table 2.

2.4.3 Cold deciduous herbaceous plants

Phenological status of cold-deciduous (annual or perennial) herbaceous plants is well captured with functions based on soil temperature (TS), while that of cold-deciduous woody plants is with air temperature (White et al. 1997). Similarly to Eqs. 1 and 4 for cold deciduous trees, the soil growing degree days ($SGDD$) of soil temperature (TS_{10}) is calculated with the base temperature constant (TS_{base}) of 0°C. Grasses generate leaves once $SGDD$ exceeds its PFT-dependent critical number ($SGDD_{crit}$) and the phenology factor for SGDD, φ_{SGDD}, becomes 1 or greater, as follows:

$$\varphi_{SGDD} = \begin{cases} \dfrac{SGDD-SGDD_{crit}}{SGDD_{length}} & \text{when } \ SGDD > SGDD_{crit}, \\ 0 & \text{otherwise.} \end{cases} \quad (6)$$

12

1 While White et al. (1997) derived $SGDD_{crit}$ as a logistic function of mean annual soil

2 temperature, here we simplify it with three different numbers for different grass types as

3 provided in Table 2. The parameters for φ_{SGDD} were fit to observations at Barrow, Alaska, for

4 arctic C3 grass; the values for C3 and C4 grasses are drawn from White et al. (1997).

5 Grasses begin fall senescence in response to decreased soil temperature. Leaves start

6 dropping once soil temperature decreases down to a given threshold, TS_{max}; grasses complete

7 senescence when soil temperature decreases further down to the critical threshold, TS_{min}:

8
$$\varphi_{TS} = \begin{cases} \min\left(1, \frac{TS_{10}-TS_{min}}{TS_{max}-TS_{min}}\right) & \text{when} \quad TS_{10} < TS_{max}, \\ 0 & \text{otherwise.} \end{cases} \tag{7}$$

9 See Table 2 for constant values of TS_{max} and TS_{min}.

10 2.4.4 Drought deciduous woody and herbaceous plants

11 Drought deciduousness depends on available soil water for the plant. In the model, it is

12 determined based on a 10-day running average of the physical time step (~half-hourly) plant

13 water stress factor β. This factor is the same used to scale stomatal conductance for water

14 stress, and is determined by a linear response between PFT-dependent critical relative soil

15 moisture (volumetric soil moisture/saturated volume) points for the plant, at which water

16 stress begins, s_*, and at which wilting occurs, s_{wilt}, (Rodriguez-Iturbe et al. 2001):

17
$$\beta = \frac{S-S_{wilt}}{S_*-S_{wilt}}. \tag{8}$$

18 $\beta=1$ when the plant is unstressed, and $\beta=0$ at the wilting point. For 6 soil layers in the LSM,

19 β is calculated for the soil moisture in each layer, and averaged weighted by layer thickness

20 and relative root mass fraction, giving the overall β experienced by the plant.

21 The phenological factor for water stress, φ_β, is determined by a linear response to the 10-day

22 running average (Foley et al. 1996) of water stress, β_{10}, to β_{max} and β_{min}, which represent

23 similarly 10-day running averages of water stress experienced before the onset of drought-

24 induced senescence and at full senescence:

25
$$\varphi_\beta = max\left(0, \left(\frac{\beta_{10}-\beta_{min}}{\beta_{max}-\beta_{min}}\right)^{\beta_{resis}}\right) \tag{9}$$

26 When β_{10} goes below a minimum (β_{min}), plants completely senesce in response to drought

27 ($\varphi=0$); when β_{10} is above a maximum (β_{max}), plants do not experience drought ($\varphi=1$); when

13

β_{10} is between β_{min} and β_{max}, the sensitivity of plants to water availability is controlled by the resistance factor (β_{resis}). The values of s_*, s_{wilt}, β_{min}, β_{max} and β_{resis} are provided in Table 2.

The leaf-on cue for drought deciduous trees is the same as that for cold-deciduous trees, while for grasses the cue is sufficient soil moisture.

2.4.5 Frost-hardening in evergreen cold-climate plants

Boreal plants undergo winter frost-hardening, which involves physiological changes to protect the plant from chilling injury and freezing injury. Following Repo et al. (1990), the state of frost hardiness S_h (°C) is modeled as follows:

$$\frac{dS_h}{dt} = \frac{1}{\tau}[(a \cdot T_{10} + b) - S_h]. \tag{10}$$

where τ is a PFT-specific time constant, and the term $a \cdot T_{10} + b$ is the stationary frost hardiness, where a and b are PFT-specific parameters for the linear relationship between stationary frost hardiness and air temperature (Hanninen and Kramer 2007). S_h can be thought of as an aggregated measure of the state of the physiological leaf processes that determine the photosynthetic capacity (Makela et al. 2004).

The state of frost hardiness is then used to adjust the maximum photosynthetic capacity $V_{c\max}$, which is an approach similar to the work of Makela et al. (2006). However, we convert from S_h to a dimensionless factor that can take values from 0 to 1. This frost hardiness factor β_{frost} is expressed as:

$$\beta_{frost} = \frac{1}{S_{h,max}}(S_h - T_0). \tag{11}$$

where T_0 is a threshold value of cumulative mean temperature at which photosynthesis starts and $S_{h,\max}$ is the maximum value of S_h (see Table 2 for constants). We implement the first-order Euler scheme to solve Eq. (10) and the resulting β_{frost} is used to adjust $V_{c\max}$.

3 Experiments

3.1 Fluxnet sites

The Ent TBM was evaluated at five Fluxnet sites, including Morgan Monroe State Forest, Harvard Forest, the Vaira Ranch, the Tonzi Ranch and Hyytiala, as briefly mentioned above

14

(Table 3). From all sites, data from the flux tower systems were available. Meteorological driver data include radiation, precipitation, air temperature, air pressure, humidity and wind, used to drive the model. Soil moisture and temperature measurements were also used to drive the Ent standalone simulations. Flux data includes net ecosystem exchange (NEE) and evapotranspiration (ET), and were used to evaluate the simulation results. Among sites, data availability, such as LAI, varied and suited different types of model simulations as described in detail in the next section.

The Morgan Monroe Sate Forest (MMSF), located in Indiana, USA (Schmid et al., 2000) (latitude: 39.32315°, longitude: -86.413139°) is is an extensive managed temperate broadleaf deciduous forest with a total area of 95.3 km^2. The area is covered primarily by a secondary successional broadleaf forest within the maple-beech to oak-hickory transition zone of the eastern deciduous forest, dominated by supar maple and tuilip poplar. LAI measurements at 5-14 day intervals during the growing season were available for 1998-2001.

Harvard Forest (latitude: 42.5313°, longitude: -72.1898°) is an eastern temperate mixed forest dominated by deciduous trees. The area surrounding the flux tower is dominated by red oak and red maple, with scattered stands of Eastern hemlock, white pine and red pine. About 1/3 of the existing red oaks were established prior to 1895, another 1/3 prior to 1930, and the rest before 1940, and thus the stand is 75–110 years old (Urbanski et al., 2007). O'Keefe (2000) provides the leaf phenology of Harvard Forest. The timings of spring leaf development and fall leaf fall have been recorded for permanently tagged individuals in the field from 1991. The leaf development and senescence data in percent of final leaf size have been used to obtain 'observational' LAI based on the maximum LAI in the model, i.e., (observed LAI) = (observed % of leaf development or fall) X (modeled maxmimum LAI).

The Vaira Ranch (latitude: 38.4066667°, longitude: -120.950733°) and Tonzi Ranch (latitude: 38.4316°, longitude: -120.9660°) in Ione, California, are located in an open grassland ecosystem and an oak/grass savanna ecosystem, respectively, in a Mediterranean climate of cool wet winters, and dry hot summers. The sites are less than 3 km apart. The grasses of both sites are C3 annual species whose growing season is during the winter to spring wet periods. Deciduous blue oaks dominate the savanna overstory of the Tonzi, with a growing season overlapping the grasses during the spring and continuing through the summer drought. In these sites, LAI measurements were available along the tower footprint for 2001 (Kiang, 2002).

15

Hyytiala (latitude: 61.8474150°, longitude: 24.294770°) in Finland is situated in needleleaf evergreen forest dominated by *Pinus sylvestris* (Scots pine), in which the phenological behavior of interest is frost-hardening. The climate is boreal. Flux measurements and soil moisture and temperature are available. For seasonal LAI, we used the site investigator's description of a constant minimum all-sided needleleaf LAI (75% of maximum) in January-May, linear increase over June to its maximum of 3.9, remaining at the maximum LAI during July-September, linear decline to its minimum in October, and a constant minimum LAI in November-December (Kolari, personal communication, 2007).

3.2 Experiment desgin

We performed a series of numerical experiments with Ent in different model modes in order to evaluate leaf seasonal dynamics, including leaf phenology and related water and carbon fluxes. We performed simulations for each site with observed soil moisture (hereafter denoted 'Ent' mode), and LSM modeled soil moisture ('LSM' mode); and with observed LAI (without allocation of assimilated carbon to growth) ('oveg') and dynamically modeled LAI (via carbon allocation) ('dveg'), giving four experiments, Ent-oveg, Ent-dveg, LSM-oveg, and LSM-dveg (Table 4). In the biophysics-only mode, the observed LAI is prescribed and related active carbon allocations are calculated according to that LAI. In the "active biomass" phenology mode, the leaf phenology and active carbon allocation are dynamically simulated. For MMSF and Harvard Forest, the model was forced with 6 and 9 years' worth of drivers, respectively. In these two sites, continuous soil moisture measurements throughout the rooting depth were not available, so only Ent-LSM simulations were performed. For Vaira, Tonzi and Hyytiala, the model was forced with a year's worth of tower-measured meteorological drivers as well as observed soil temperature and moisture.

For the Ent versus LSM simulations for annual grass phenology, it was necessary to tailor the soil moisture stress parameterst to the different metrics of soil moisture. The phenological timings of grasses depend on the soil moisture condition while an LSM-derived soil moisture is a model-specific index of soil wetness, not a physical quantity that can be directly validated with field measurements (Koster et al., 2009). The thresholds for the root water stress factor (β in Eq. 8) that was used to model drought-deciduous behavior of grasses (volumetric soil moisture at onset of stress and at wilting point) were derived from the observed soil moisture and fluxes, such that these parameters were in a sense tuned to the site as well as to the type

16

of soil moisture measurement. In this study, we therefore tuned the parameters for LSM to better capture the phenological behaviors.

For diagnostics for model performance, we examined observed monthly LAI, and monthly sums of gross primary production (GPP), ecosystem respiration (R_E), net ecosystem productivity (NEP = GPP - R_E) and total evapotranspiration (ET). For potentially water-limited sites, we examined the modeled volumetric soil moisture and Ent's plant water stress factor. For observed R_E, the values are inferred from nighttime respiration and its sensitivity to soil temperature, while the modeled values result from both autotrophic and soil respiration. Soil carbon as a driver of soil respiration was initialized from site measured soil carbon, with litterfall from the model as inputs on a daily basis (soil carbon was not driven to equilibrium).

4   Results

4.1   Cold deciduous woody plants

4.1.1 Phenology

We evaluated the model performance for cold deciduous woody plants at two sites, Morgan-Monroe State Forest (MMSF) in Indiana, and Harvard Forest.

Figure 3 and Table 5 show the simulated variations of the phenological factor (ratio of LAI to the maximum LAI of the year) in comparison to observations. First, it is clear that the gradual nature of changes in LAI during spring and fall were not captured in the model. The phenological factor serves as an on-/off cue between environmental thresholds, while growth rate with the ED scheme is limited only by carbon availability, for which reserve carbon is generally not limiting in trees (Sala et al. 2012) or in grass seeds (William Parton, pers. communication). At both sites, the inter-annual variations of leaf-on timings in the spring were better captured than those of the leaf-off timings in the fall. At Harvard Forest, the dates with the elongation factor of 0.5 in spring showed a correlation coefficient (R) of 0.85 and a root mean squared error (RMSE) of 3.00 days, while the dates with an elongation factor of 0.5 in fall showed R of 0.04 and an RMSE of 15.09 days.

17

4.1.2 Fluxes

In MMSF, the predicted NEP reasonably followed the observed NEP (Schmid et al. 2000, Dragoni et al. 2007) with correlation coefficients ranging from 0.86 to 0.94, while the peak NEP in summer was slightly underestimated compared to the observed (Fig. 4 and Table 6). However, both GPP and R_E were both more extreme in the model compared to the Fluxnet data product.

In Harvard Forest, the default simulations (LSM-dveg and LSM-oveg) showed underestimated NEP compared to the flux tower observations due to simulated water stress (Fig. 5). As it is known that the cold deciduous plants in Harvard Forest do not experience water stress, no root water stress ($\beta = 1$ in Eq. 8) is assumed for additional simulations (LSM-dvegNS and LSM-ovegNS). With the prescribed water stress factor of 1, the model captured the observed NEP reasonably and overestimated GPP and RE compared to observations, similar to MMSF simulations.

The ET in both LSM simulations were overestimated compared to the flux tower observations in MMSF and Harvard Forest. These discrepancies might be attributed to both model and data errors. In the model, the higher estimated GPP (although we cannot confirm this) may lead to the overestimated ET to some extent, since higher photosynthesis corresponds to higher canopy conductance and hence more transpiration. In addition, it is well known that eddy flux measurements do not close the energy balance (Wilson et al. 2002). The sum of latent, sensible and ground heat is generally smaller than the net shortwave radiation, which is often caused by measurement errors of latent heat (i.e., ET) and sensible heat (Aranibar et al. 2006), leading to imbalance in measured net radiation of as much as 20%. The LSM simulated peak ET is within approximately 70% of measurements.

4.2 Drought deciduous herbaceous plants

4.2.1 Phenology

We evaluated the model performance for drought deciduous herbaceous and woody plants at two sites, the Vaira Ranch and Tonzi Ranch in California. As shown in Fig. 6, at both sites, the timings of C3 annual grasses' green-up and senescence are mainly controlled by soil moisture in a Mediterranean climate, in which precipitation and temperature are seasonally out of phase. Grasses are active during the winter rains, but slightly cold limited in activity,

18

then with spring warming, growth and activity increase, followed by rapid senescence that closely tracks soil moisture dry-down in the late spring, and full senescence by the beginning of the dry, hot summer. At the Tonzi Ranch, the oaks have the opposite seasonality to the C3 grasses. The oaks leaf out at the end of winter rains around March, when grasses have reached their peak, and then the trees start gradually losing their leaves around the beginning of July due to drought stress. Their complete leaf-off appears to be cued by November cold or fog, but this latter cue would not be considered a stress factor and is not well understood.

At both Vaira and Tonzi Ranches, Ent-dveg and LSM-dveg reasonably captured these phenological timings (Fig. 6). The growth rate for herbaceous plants (i.e., increase in LAI during the growing season) reflected the net carbon assimilation each day, and slightly lagged observations at the beginning of the growing season in the model. Simulated soil moisture clearly decreased much more slowly in LSM-dveg during the late spring dry-down compared to the observed volumetric soil moisture that was used to drive Ent-dveg.

4.2.2 Fluxes

For carbon fluxes at the Vaira Ranch, the model simulations generally followed the observed seasonality, although the late leaf-off in LSM-dveg leads to overestimation of carbon uptake significantly, and the observed abrupt increase in R_E in the beginning of the growing season was not captured in all cases (Fig. 7 and Table 6). Xu and Baldocchi (2004) suggest that the large pulse of R_E is the consequence of quickly stimulated microbial activity in decomposition after rain events during the dry season. In the Ent TBM, the soil moisture dependency of decomposition is parameterized as a linear function of soil saturation percent (S) with a plateau when $S > S_{opt}$ (70%). This response is derived from raw data of soil respiration responses to temperature and moisture in grassland and winter wheat soils from Del Grosso et al. (2005). Most likely, the damped response is because the Ent TBM does not model a separate litter layer on top of the soil, and litter quality may not be well parameterized to allow for fast turnover. As this is a soil model issue, further analysis is worthy of a separate study.

At the Tonzi Ranch, the simulated NEP resulted in an RMSE of ~0.4 $\mu mol/m^2/s$ compared to the observed flux (Fig. 7 and Table 6). During the late spring soil moisture dry-down period, the grasses senesced and the oaks retained their leaves. The oaks started reducing their carbon assimilation due to water stress, as the Ball-Berry slope (m; slope for stomatal

19

conductance) is scaled linearly with the water stress in the model. In reality, the oaks at Tonzi adjust their osmotic potential to maintain their water potential, so their leaf water potential is not linear with soil moisture (Kiang 2002). Therefore even with the reasonable LAIs in Ent-oveg, Ent-dveg and LSM-dveg, the underestimated NEP and GPP in the summer are to be expected, lacking a non-linear response function. Meanwhile, the overestimated LAI in LSM-dveg clearly led to overestimated NEP and GPP. Furthermore, we found the soil biogeochemistry model did not capture the soil respiration pulses after the rainfall, as in Vaira.

The model reasonably captured the observed seasonality of ET with an R of ~ 0.9 in Vaira and ~ 0.8 in Tonzi, while the R values for carbon fluxes were much lower. The water fluxes were not much different between LSM-dveg vs. LSM-oveg, while the carbon fluxes were significantly different due to different LAIs between the two. The differences in transpiration, resulting from different LAIs, were compensated by evaporation, leading to a relative small discrepancy in ET between the two experiments. Furthermore, the amplitudes (difference between the maximum and the minimum) of ET were clearly damped in the model, with underestimated peak fluxes during the growing season and overestimated fluxes during the non-growing season. In particular, the noticeable amount of ET occurred during the non-growing season in Vaira, suggesting the partitioning of ET into evaporation and transpiration should be further investigated.

4.3 Frost-hardening in evergreen cold-climate plants

4.3.1 Phenology

At Hyytiala, the phenological behavior of interest is frost-hardening, which lowers photosynthetic capacity in the winter. In comparison to observed LAI, assumed according to Kolari (personal communication, 2007) as explained in Section 3.2, simulated LAIs (Ent-dveg and LSM-dveg) (Fig. 8) were almost constant at 4 m^2/m^2 throughout the year, without much decrease during the winter. For evergreen plants, LAI variations in the model reflect the change in foliage carbon balance, as the phenological factor for evergreens remains 1 all the time. Thus, the relatively constant LAIs mean no significant carbon losses during the winter in the model. Based on additional Ent-dveg and LSM-dveg without frost-hardening (not shown), we found that such discrepancy in LAI between observation and simulation itself did not influence the predicted water and carbon fluxes noticeably.

20

4.3.2 Fluxes

Modeled frost-hardening in the spring improved the predicted seasonality of NEP markedly in both Ent and LSM simulations (Fig. 8 and Table 6). Frost-hardening suppressed photosynthetic capacity during the winter (particularly in Feb-April) and therefore GPP and NEP. It also suppressed transpiration and thus ET, but a relatively small difference in ET was detected between the simulations with and without the frost-hardening scheme as the RMSEs with observations were 7.88 mm/s and 7.89 mm/s, respectively (Table 6).

With regard to the differences between the Ent-standalone and Ent-LSM models (Ent-dveg vs. LSM-dveg), we found the magnitude of NEP was overestimated in Ent-dveg due to high simulated GPP and underestimated in LSM-dveg due to low soil moisture. During the growing season, the observed volumetric soil moisture was above ~0.35 m^3/m^3, and the resulting root water stress factor was 1 (completely unstressed) most of the time in Ent-dveg (driven with the observed soil moisture and temperature). However, the predicted volumetric soil moisture was below ~0.25 m^3/m^3 during the growing season in the top 3 soil layers and the plants roots experienced an average water stress factor of 0.68. Such underestimated soil moisture in the Ent-LSM led to low estimates of NEP.

5   Discussion

Our experiments show that phenological timing of leaf-out and senescence can be fairly well captured within 10 days or better of observations for deciduous or annual vegetation when based on cumulative weather statistics (air and soil temperature, growing degree days, day length) derived from observations in the literature. However, the response to soil moisture is sensitive to whether deep root water access is represented to offset soil moisture stress in shallow soil. Also the soil moisture response must be tuned to the given measure or land model, because soil water content as simulated at the spatial resolution of a land surface hydrology model does not correspond well with any field measure of soil moisture (e.g. volumetric water content, matric potential, pre-dawn water potentials). Stomatal conductance and soil respiration are sensitive to soil moisture stress and hence subject to inaccuracy dependent on the soil moisture representation. Meanwhile, we uncovered weaknesses in the representation of particular vegetation processes – autotrophic respiration and ED-based

carbon allocation – that, besides differences in simulated LAI at one site, were the primary causes of differences from observed NEP.

5.1 Drought deciduousness

In Vaira grassland and Tonzi savanna, the phenology parameters, which are based on the plant water stress factor (a function of soil moisture), were derived from the site observations of volumetric soil water content (Eq. 8), and they perform well with observed soil moisture in Ent but not with simulated soil moisture in the LSM. The GISS LSM model predicted the same seasonal trends of soil moisture but higher in magnitude and lower in variability than observations. Koster et al. (2009) point out that simulated soil moisture is a model-specific quantity and thus that can be considered as an "index" of the moisture state. The specific evaporation and runoff formulations, in addition to model-specific soil parameters such as porosity, hydraulic conductivity, wilting point and layer depth defines a dynamic range of soil moisture simulated by the certain model. Therefore the true information content of soil moisture data lies not necessarily in their absolute magnitudes but in their time variability.

Therefore, the current approach using the absolute soil moisture value for water-limited phenology parameterization could be improved by properly mapping the soil moisture values from the field sites into those in the model, or by using the surrogates for the soil moisture, such as VPD as suggested by Jolly et al. (2005). However, Stöckli et al. (2011) note that VPD may not be a good indicator of deep soil moisture.

For the trees at MMSF and Harvard Forest, LSM-simulated water stress where the plants should be unstressed indicates that calculating the water stress factor by weighting by root depth distributions does not accurately reflect how trees actually access water. Deep roots generally supply water when shallow layers are dry, and many trees perform hydraulic lift. A future revision of the Ent water stress scheme will account for the ability of plants preferentially to access soil moisture at any depth in the root zone, such that soil moisture stress is not a simple weighted average through the root profile.

While the Fluxnet data have been widely used to evaluate the DGVMs and LSMs recently, we still found the need for more comprehensive measurements at the sites. Specifically, it was very difficult to have continuous soil moisture and temperature together along with measurements with eddy covariance towers; also the detailed tree surveys were not always available.

22

5.2 Cold deciduousness

For cold deciduous trees, we used the growing degree days and chilling requirements in spring phenology (Botta et al., 2000) and temperature and photoperiod in fall phenology (White et al., 1997; Jolly et al., 2005). While we have taken a widely used approach, some recent studies suggest other possible approaches. For spring phenology, the importance of photoperiod has been pointed out in recent studies (e.g., Korner and Basler, 2010; Migliavacca et al., 2012). Korner and Basler (2010) suggested that when the chiling requirement is fulfilled, plants become receptive to photoperiod signals and such sensitivity to photoperiod is found in late sucessional species in mature forests. For fall phenology, Delpierre et al. (2009) used chilling degree day-photoperiod to model leaf coloring change for deciduous trees in France, and Yang et al. (2012) and Archetti (2013) found the model suitable for New England, US, with different parameter fits. In general, despite agreement about overall climate cues for cold deciduousness, further work is needed to uncover site-independent parameterizations.

5.3 Photosynthesis and respiration parameters

In this study, site-specific parameters were used according to the data availability. As in Appendix D, some of parameters are generic for PFTs and some are site-specific. For the model to be utilized at the global scale, further exploration is required to determine geographic variation in and possible climatology-based prediction of parameters. Model parameters for biophysics or ecosystem models have been inferred with various mathematical techniques, such as a Monte Carlo simulation (Kleidon and Mooney 2000), data assimilation with Kalman filtering (Mo et al. 2008, Stöckli et al. 2008), optimization with the Marquardt-Levenberg method (Wang et al. 2007), and optimization with Simulated Annealing method (Medvigy et al. 2009, Kim et al. 2012).

In general, vegetation biophysics models can replicate observed canopy fluxes of CO_2 well when the vegetation structure is well-specified, but the same net flux can be predicted from different levels of gross assimilation versus respiration. The main biophysical parameters common to most models are the maximum leaf photosynthetic carboxylation rate, Vcmax; autotrophic respiration as a function of biomass, temperature, and activity; and leaf litter quality, such as lignin content, for soil respiration. While Vcmax may be precisely measured for a leaf, its value can be highly variable within a plant and seasonally. Currently in the Ent

23

model, Vcmax is only variably with PFT and temperature, and the intrinsic quantum efficiency for Jmax is constant. The seasonal variation of Vcmax, Jmax, and SLA could be introduced, pending better mechanistic understanding. A simple approach based on photoperiod such as in Bauerle et al. (2012) would be possible.

Autotrophic respiration can range ~30-80% of annual GPP for different plant types (Falge et al. 2002). These parameters, however, may not extrapolate to the global scale, and thus future study is necessary to investigate global variation in parameterizations. In general, respiration is poorly understood and cannot be modeled fully mechanistically, but must rely on bulk parameterizations that effectively integrate numerous processes. Researchers have attempted various approaches to grouping some respiratory fluxes (Amthor 2000, Cannell and Thornley 2000) as responsive to different drivers, though there is as yet no generally accepted scheme. In Ent, the streams are maintenance respiration that is a function of biomass and responsive to temperature, "light growth respiration" from photosynthetic activity, and "biosynthesis respiration" from growth or turnover of plant tissues.

In Ent, using site-specific parameters for leaf photosynthetic capacity, Vcmax, constant throughout the canopy, we observed a tendency toward higher GPP and higher ecosystem respiration, R_E, compared to that inferred from tower observations when night-time respiration temperature response is used to estimate R_E. These extremes in the two components of the net flux are not necessarily unreasonable, since the Fluxnet respiration product could be underestimated. The R_E data products we used were modeled, as typical, with an exponential equation to fit the measured night-time CO_2 flux as a function of soil temperature (Schmid et al. 2000). Such an estimate excludes daytime root respiration, which increases with photosynthetic activity (Tang and Baldocchi 2005, Tang et al. 2005). With regard to GPP, recent oxygen isotope work suggests that global gross primary productivity is higher than traditional estimates (Welp et al. 2011). It is a well-known problem in ecosystem science that GPP and respiration cannot be directly partitioned through current measurement methods for net ecosystem exchange, although there are hopes for a solution now possibly with measurements of solar-induced fluorescence (van der Tol et al. 2014).

5.4   Carbon allocation/growth scheme

We encountered deficiencies in the carbon allocation/growth scheme that we adopted from the ED model. Although the current carbon allocation and growth scheme results in LAI that

is reasonable, with some phenological timing issues as noted, the maximum LAI is achieved thanks to a cap on LAI by allometric relations to stem structure and plant density, while the rest of the plant carbon balance is not realistic, particularly with regard to rate of LAI growth, amount of seasonal sapwood growth and conversion to heartwood, accumulation of carbon reserves, and allocation to reproduction. The on/off cues of the Ent phenological factor for cold deciduous trees results in unrealistic fast full leaf-out, which could be rectified by introduction of a physically-based cell growth elongation factor (Lockhart 1965). We also found it would be more realistic to make carbon allocation to each live pool independent. The ED scheme's allocation to one live biomass total and then partitioning among the live pools can lead to unrealistic behaviors for sapwood patterns during spring growth and fall senescence, due to a partitioning scheme for live carbon that does not account for the different seasonal behaviors of each live pool. Finally, reproduction in ED currently is a fixed fraction of assimilated carbon, which is problematic in the plant's overall carbon balance as a large sink. Recent studies show that reproduction relies heavily on stored carbon, which often accumulates over more than a year, such that growth of other plant tissue is never carbon limited while large stores are kept in reserve. The ED scheme relies on the plant using nearly all stored carbon for deciduous plants each year. Introducing reproductive allocation based on thresholds proposed by Sala et al. (2012) would help rectify Ent's simulated plant carbon balances such that trees are not always reaching the limit of carbon starvation. Besides respiration, plant carbon allocation is currently still poorly understood. However, recent studies with carbon tracers (Epron et al. 2012, Epron et al. 2012) are yielding new insights that could be used to improve growth schemes that continue to be a weakness in dynamic global vegetation models.

6   Conclusions

In this study, we evaluated the Ent TBM focusing on the seasonal dynamics of vegetation leaf as well as carbon and water fluxes. In particular, we took a process-based approach, evaluating the Ent-standalone model with observed LAI and Ent's prognostic active growth submodel with observed soil moisture as well as coupled to the LSM model for prognostic soil moisture, allowing us to identify parameterizations that need to be improved. For herbaceous PFTs whose phenological timings depend on soil water availability, it is inevitable to find errors in phenological timing in Ent-LSM simulations due to the

KIANG, NANCY Y. …, 10/30/15 11:20 PM
Deleted: the need

KIANG, NANCY Y. …, 10/30/15 11:20 PM
Deleted: would be more realistic

Yeonjoo 9/30/15 10:31 PM
Deleted: found that the

Yeonjoo 9/30/15 10:33 PM
Deleted: awkward and

Yeonjoo 9/30/15 10:31 PM
Deleted: Making carbon allocation to each live pool independent would be more realistic.

discrepancy in simulated soil moisture in the LSM. Also the predicted LAI of herbaceous PFTs in Ent directly reflects the amount of assimilated carbon on the day and vice versa as herbaceous PFTs allocate assimilated carbon only to active compartments (as they have no structural tissue), and thus any errors in phenological timings propagate into errors in biophysical processes.   For tree PFTs, the Ent soil moisture stress scheme should be improved to allow deep soil moisture access to override stress that might result from weighting shallower dry soil layers too strongly.

This study evaluated the phenology and resulting seasonality of fluxes in the limited number of sites, including 4 different PFTs. The Ent PFTs not tested in this study include deciduous needleleaf plants, evergreen broadleaf plants, shrubs, arctic grasses and crops. Future work will involve determining the efficacy of these PFT parameterizations at the global scale, and the possibility of developing some of these parameters as functions of local climate as obtained from either reanalysis data or from GCM climatology. In addition, we have identified deficiencies in the carbon allocation scheme from the ED model that can be rectified in future revision of Ent's growth submodel.

Future work will include development of phenology and allometry parameter sets that are robust at the global scale, and soil moisture stress accounting for deeper soil access. In addition, due to how ED allocates biomass to all live pools (foliage, sapwood, fine roots) combined rather than allowing for separate dynamics, alternative carbon allocation schemes that partition the dynamics of the live tissues must be developed for realistic plant carbon balances.

This work sets the foundations for coupled land carbon-GCM simulations that can utilize height-structured canopy data from remotely sensed lidar, to reduce uncertainty in predictions of the land carbon balance through tighter links between seasonal growth dynamics geometrical and biomass allometry of vegetation canopies. Because use of the model at the global scale will involve community users who will continue to identify parameter sets applicable for more climatically diverse distributions of the Ent TBM's plant functional types, this paper is also written to serve as a detailed reference for these users for appropriate interpretation of model results and parameter adjustment.

Appendix A: Root profiles

Depth profiles of root density are modifications of those in (Rosenzweig and Abramopoulos 1997), revised to fit the PFT categorizations in the Ent TBM. These are modeled as cumulative normalized root density distributions $F(z)$ of a PFT as:

$$F(z) = a_{PFT} Z^{b_{PET}} \qquad\qquad (A1)$$

where z is soil depth (m), and a and b are PFT-specific parameters, summarized in Table A1. The cumulative distributions are plotted in Since soil layers in the NASA GISS land surface model only are defined down to 3.5 m depth, maximum root depths are limited to this value.

Appendix B. Soil biogeochemistry in the Ent Terrestrial Biosphere Model

The soil biogeochemistry submodel of Ent is utilizes a slightly modified version of the CASA' biosphere submodel originally implemented in the NCAR LSM and CSM 1.4 (Bonan, 1996; Randerson et al., 1997; Fung et al., 2005; Doney et al., 2006), which itself is a modified version of the original NASA-CASA biosphere model (Potter et al., 1993). The soil model determines terrestrial soil carbon pools and CO_2 fluxes from microbial respiration.

B.1. CASA structure

The soil biogeochemistry model consists of 3 litter C and N pools and 9 soil C and N pools, as in CASA'. The pools currently are only simulated for the top 30 cm soil depth. This layer accounts for nearly all observable soil respiration fluxes to the atmosphere, but not for full long-term carbon stocks in deeper soil. Down to 100 cm and deeper would allow comparison to existing global datasets of soil carbon and root depths (Batjes, et al., 1996ab; Jackson, et al. 1996). Appendix Figure B1 shows these 12 pools. Ent has an optional 30-100 cm deeper soil layer that is not run in the current paper.

The various pools currently have fixed C:N ratios and turnover times, listed in Table B1. The pools gain carbon and nitrogen from transfers from other pools, and losses to respiration and transfers to other pools. These transfer and respiration fractions are listed in Table B2.

Soil micrometeorological conditions for the soil layers must be extrapolated from the soil layering scheme of the land surface model. For example the GISS land surface hydrology has a 6-layer soil scheme with geometrically increasing layer thicknesses with depth (Rosenzweig &

27

Abramopoulus, 1997), so soil temperature and moisture for the soil biogeochemistry layers are calculated through a weighted sum for the upper 30 cm.

In addition to the transfer coefficients in Table B2, three other rate coefficients are used (following Randerson et al., 1997):

fact_soilmic = 1.25;

fact_slow = 1.5;

fact_passive = 1.5.

These are simply decomposition rate adjustment factors for soil microbial, slow, and passive pools (respectively) *for crops only*; their values for all other PFTs is 1.

B.2. Soil module interface with vegetation

Physical inputs to the soil module from the land surface hydrology are volumetric soil moisture, soil temperature, and soil texture (percentage of clay, sand, and silt). Biological inputs consist of leaf, root, and wood litter (Figure B1). Model outputs are soil C (and N, not used) pools and soil CO_2 flux. Ent calculates litterfall carbon from the leaf area times the specific leaf area,

The relevant plant functional type (PFT)-dependent litter parameters (leaf, fine root, and wood turnover times, litter C:N ratios, specific leaf area, and lignin contents) from Ent are listed in Table B2. In addition to these parameters, a parameter representing the inverse of the residence times of the litter pools, denoted $annk_{lit}$ (in units of yr^{-1}), was calculated as the inverse of lrage for leaf and root litter or of woodage for wood litter (Potter et al., 1993).

B.3. Temperature and moisture responses of soil respiration

We replaced the CASA' temperature and soil moisture responses of soil respiration with new functions derived from new fits to field data collected by Del Grosso et al. (2005). The Ent TBM temperature response of soil respiration is a simple piece-wise linear model that increases up to 30 °C, then flattens. In reality, the response to temperature is exponential up to a certain optimum then declines, but a linear representation was chosen because it reduces the computational time compared to that required for calling an exponential function, and tests on field data show adequate performance for the purpose of predicting respiration fluxes and soil carbon pools (unpublished). At high soil temperatures, soil moisture stress usually

28

occurs also, but because no measurement data were available for respiration at temperatures above 30 °C, the Ent model response does not represent a decline in soil respiration at high temperature. The linear temperature response of soil respiration is:

$$\text{linear } f_{temperature} = \begin{cases} Intercept = 0.04607913, \; Tsoil \leq 0°C \\ \dfrac{(1 - Intercept)}{(30 - 0)} T_{soil} + Intercept, 0 < Tsoil \leq 30°C \\ 1, \quad T_{soil} \geq 30°C \end{cases}$$ (B1)

More realistically, the temperature response is in nature an exponential response, so if there are no computational constraints, the following Q10 function as formulated in the orignial CASA' should be used:

$$\text{exponential } f_{temperature} = Q10^{\frac{T_{soil,C} - 30.0}{10.0}}$$ (B2)

where Q10 has a typical value of 2.0.

The Ent TBM moisture response of soil respiration is similarly a piece-wise linear model that rises from 0 at zero soil moisture to 1.0 at a relative extractable water content (REW) of 0.7, where REW is the fraction of saturation above the hygroscopic point. Because there are no good functions for calculating hygroscopic point based on soil texture, we estimate the hygroscopic point as half of the wilting point. We note that it would be more precise to model the soil moisture response as an optimality curve, that rises from the soil hygroscopic point (minimum for microbes) rather than wilting point (for plants) to some optimum, then declines as pore space becomes saturated and obstructs the flux of gases. However, lack of good algorithms to calculate the soil hygroscopic point for different soil textures necessitate this version of Ent relying on the wilting point as the point of minimum available soil moisture. We may later introduce a simple linear decline of the soil moisture response with saturation, but at present we have no data on the response to saturated conditions.

$$f_{moisture} = \begin{cases} 0, \quad REW \leq 0 \\ \dfrac{1}{0.7} REW, \quad 0 < REW \leq 0.7 \\ 1, \quad REW \geq 0.7 \end{cases}$$ (B3)

The linear soil respiration temperature and moisture response functions are plotted in Appendix Figures B1 and B2, along with the original CASA' responses, and those of Del Grosso et al. (2005), whose data were re-analyzed to generate the Ent response functions.

Appendix C: Allocation

The labile carbon reserves in Ent are allocated into different plant biomass pools, including foliage, sapwood, heartwood, fine root and coarse root. In addition, turnover of tissue due to background litter fluxes is replenished from the carbon reserve pool. In nature, plants may allocate biomass to different compartments in response to many different controlling factors, such as light availability and water availability, which alter, for example, root:shoot ratios. Among various carbon allocation modeling approaches with different complexities, many DGVMs take a simple approach to model carbon allocation via empirical and allometric relationships, a traditional 'static allocation' approach (Foley et al. 1996, Sitch et al. 2003) while some models parameterize the dependency of carbon allocation on resource availability, 'dynamic allocation' approach (Friedlingstein et al. 1999, Arora and Boer 2005). Although carbon allocation varies with plant status such as size and age, and environmental conditions, the static allocation approach may be justified for models operating at the large scale. If plant productivity is assumed in a steady state, carbon allocation is likely to be in a steady state. Also, spatial variability in environmental factors and their effects on allocation can be averaged. However, the fixed allocation approach is limited in long-term simulations as it lacks response to environmental changes such as climate change and elevated atmospheric CO_2 (Franklin et al. 2012). However, recent models of 'dynamic allocation' have been difficult to constrain due to a dearth of observations.

In the Ent TBM, the allocation submodel takes a traditional approach of 'static allocation', based on allometric relationships between different pools. Modified from approaches of the ED models (Moorcroft et al. 2001, Medvigy et al. 2009), the scheme allocates the labile carbon to different biomass pools according to empirical allometric relationships and leaf phenological status on a daily basis.

C.1. Active biomass

1   The biomass within each plant is partitioned between an active carbon pool and a structural

2   carbon pool. The active biomass pool (B_{active}) (kg$_{biomass}$/cohort) is sub-divided into foliage

3   (B_{fol}), sapwood (B_{sw}) and fine roots (B_{froot}) which turn over at different rates, while the

4   structural pool ($B_{structural}$) consists of heartwood (B_{hw}) and coarse roots (B_{croot}). Grasses do not

5   have the structural pool. The labile biomass (B_{lab}) assimilated on the same day is allocated to

6   the active carbon pool to maintain the size of foliage, sapwood and fine root tissues given

7   their turnover rates, and to accumulate the active carbon up to its maximum.

8   Thus, the time change of the active pool can be written by

9    $$\frac{dB_{active}}{dt} = \min\left[\min(B_{lab}, CB_d), B_{active}^{max} - B_{active}\right] \qquad (C1)$$

10   where $B_{active}{}^{max}$ is the maximum active carbon of each plant, which is determined according to

11   the maximum foliage carbon according to the size of plant, CB_d is the daily plant carbon

12   balance (i.e., sum of NPP on one day). Then, the allometric relationships are used to sub-

13   divide the active biomass into its components. The foliage biomass is determined according

14   to its phenological status (φ), ranging from 0 (for full senescence) to 1 (full leaf-out), as a

15   proportion of full-leaved foliage biomass, $B_{fol}{}^{*}$, so that $B_{fol}=\varphi\ B_{fol}{}^{*}$. Both the fine root and

16   sapwood biomass are also determined according to their proportional relationships to $B_{fol}{}^{*}$. A

17   constant empirical proportionality for fine root (q_{fr}), assumed to be 1, is related as:

18   $$q_{fr} = \frac{B_{froot}}{B_{fol}^{*}} = 1 \qquad (C2)$$

19   The sapwood biomass is determined according to the pipe-model theory (Shinozaki et al.

20   1964), which suggests that the total foliage area is proportional to the sapwood cross-sectional

21   area. The ratio between full-leaved foliage area and sapwood area is assumed to be 3900

22   (m^2$_{foliage}$/m^2$_{sapwood}$). This value is adopted from the value used in ED1 (Moorcroft et al. 2001),

23   which follows Rending and Taylor (1989), giving the ratios of foliage area to sapwood area

24   ranging from 3900 to 14000. These assumptions result in the following relationship:

25   $$\frac{\text{(foliage area)}}{\text{(sapwood area)}} = \frac{SLA \cdot B_{fol}^{*}}{\frac{B_{sw}}{\rho_{sw} \cdot h}} = 3900 \qquad (C3)$$

26   where ρ_{sw} is the sapwood density (kgC/m^3$_{sapwood}$) and SLA is the specific leaf area

27   (m^2$_{foliage}$/kgC) for each PFT, provided in Table 1. ρ_{sw} is taken to be 500 (kgC/m^3$_{sapwood}$) (i.e.,

28   0.5kgC/kg$_{biomass}$ x1000 kg$_{biomass}$/m^3$_{sapwood}$ for very hard wood). However, we note that there

29   are departures from these constant values. The fraction of dry biomass that is carbon in

Yeonjoo 9/7/15 9:50 AM
Deleted: B1

Yeonjoo 9/7/15 9:50 AM
Deleted: B2

Yeonjoo 9/7/15 9:50 AM
Deleted: B3

1   spruce wood is typically 0.48 (Payne 2002). Also, Schneider et al. (2011) find the foliage to

2   sapwood area ratio to be closer to 500-600 for Jack pine, with higher values toward the

3   interior of the sapwood that serves older foliage. Calvo-Alvarado et al. (2008) find an

4   increasing linear relation between height and foliage area/sapwood area for Costa Rican

5   rainforest trees, ranging from 500-1500. A consistent rule for this variation has yet to be

6   identified, but it may vary with wood density and anatomy.

7   Finally, B_{fol} is related to LAI ($m^2_{foliage}/m^2_{ground}$), measuring the total leaf (i.e., foliage) area per

8   the projected ground area by

9    $$LAI = 0.5 \cdot B_{fol} \cdot SLA \cdot nplant \qquad \text{(C4)}$$

10   where *nplant* is the population density of cohorts (# plants/m^2_{ground}), and 0.5 (kgC/kg$_{biomass}$) is

11   to convert SLA in $m^2_{foliage}$/kgC to $m^2_{foliage}$ /kg$_{biomass}$.

C.2. Structural and reproductive biomass

13   Growth of structural tissue is handled as follows. If the stored labile biomass is non-zero, the

14   size of the structural pool of woody plants increases according to the empirical allometric

15   relationships and consequently the size of the active pool increases. Here, the partitioning

16   between B_{active} and $B_{structural}$ is written by

17    $$q_{structural} = \frac{dB_{structural}}{dB_{active}} = \frac{\frac{dDBH}{dB_{active}}}{\frac{dDBH}{dB_{structural}}} \qquad \text{(C5)}$$

18   where *DBH* is the diameter at breast height and $q_{structural}$ is the ratio of structural growth to

19   active growth. The derivatives are derived from allometric relationships according to plant

20   size (i.e., DBH, and height) for woody plants. Note herbaceous plants do not have the

21   structural pool, meaning that *DBH*=0, $q_{structural}$=0, $B_{structural}$=0, and q_{sw}=0. Also, the plant

22   devotes a fixed fraction (q_{repro}) of daily carbon to the reproductive pool and the rest to growth

23   of the active and structural pools. q_{repro} is assumed to be 0.3 for woody plants and 1.0 for

24   herbaceous plants, following the assumptions of ED1 (Moorcroft et al. 2001).

Yeonjoo 9/7/15 9:50 AM
Deleted: B4

Yeonjoo 9/7/15 9:50 AM
Deleted: B

Yeonjoo 9/7/15 9:50 AM
Deleted: B5

Appendix D: Biophysics, Allocation, and Phenology Parameters

See Table D1 and D2.

Code Availability

The Ent TBM is being developed as a part of NASA GISS ModelE. Version 1.0.0.0.0, Ent biophysics, is available in http://data.giss.nasa.gov/modelE/ (Schmidt et al, 2014). As noted in the main text, users of this version of Ent phenology and growth, version 1.0.1.0.0, are encouraged to use it for site-based studies with parameters derived at the site level, not for global studies. Since Ent TBM v1.0.1.0.0 does not yet apply at the global scale, it is not released yet in ModelE for GCM use, but the code used in this study may be obtained by contacting the corresponding author via email.

33

References

Abramopoulos, F., Rosenzweig, C., and Choudhury, B. J.: Improved ground hydrology calculations for global climate models (GCMs): soil water movement and evapotranspiration, J. Climate, 1, 921–941, 1988.

Amthor, J. S.: The McCree–de Wit–Penning de Vries–Thornley respiration paradigms: 30 years later, Ann. Bot.-London, 86, 1–20, 2000.

Aranibar, J. N., Berry, J. A., Riley, W. J., Pataki, D. E., Law, B. E., and Ehleringer, J. R.: Combining meteorology, eddy fluxes, isotope measurements, and modeling to understand environmental controls of carbon isotope discrimination at the canopy scale, Glob. Change Biol., 12, 710–730, 2006.

Arora, V. K. and Boer, G. J.: A parameterization of leaf phenology for the terrestrial ecosystem component of climate models, Glob. Change Biol., 11, 39–59, 2005.

Badeck, F. W., Bondeau, A., Böttcher, K., Doktor, D., Lucht, W., Schaber, J., and Sitch, S.: Responses of spring phenology to climate change, New Phytol., 162, 295–309, 2004.

Baldocchi, D., Falge, E., Gu, L., Olson, R., Hollinger, D., Running, S., Anthoni, P., Bernhofer, C., Davis, K., Evans, R., Fuentes, J., Goldstein, A., Katul, G., Law, B., Lee, X., Malhi, Y., Meyers, T., Munger, W., Oechel, W., Paw U, K. T., Schmid, H. P., Valentini, R., Verma, S., Vesala, T., Wilson, K., and Wofsy, S.: FLUXNET: a new tool to study the temporal and spatial variability of ecosystem-scale carbon dioxide, water vapor, and energy flux densities, B. Am. Meteorol. Soc., 82, 2415–2434, 2001.

Baldocchi, D., Xu, L. K., and Kiang, N.: How plant functional-type, weather, seasonal drought, and soil physical properties alter water and energy fluxes of an oak-grass savanna and an annual grassland, Agr. Forest Meteorol., 123, 13–39, 2004.

Ball, J., Woodrow, L. E., and Beny, J. A.: A model predicting stomatal conductance and its contribution to the control of photosynthesis under different environmental conditions, in: Progress in Photosynthesis research, edited by: Biggins, J., Nijhoff, Dordrecht, 221–224, 1987.

Batalha, N. M., Rowe, J. F., Bryso, S. T. et al.: Planetary candidates observed by Kepler, III: Analysis of the first 16 months of data, The Astrophysical Journal Supplement Series, 204, 24 (21 pp.), doi:10.1088/0067-0049/204/2/24, 2012.

Batjes, N. H.: Total carbon and nitrogen in the soils of the world, European Journal of Soil Science, 47, 151-163, 1996.

Batjes, N. H.: Documentation to ISRIC-WISE global data set of derived soil properties on a 1/2 deg by 1/2 deg grid (Version 1.0), Wageningen, The Netherlands., International Soil Reference and Information Centre (ISRIC), 1996.

Bonan, G. B.: A land surface model (LSM Version 1.0) for ecological, hydrological, and atmospheric studies: technical description and user's guide, Boulder, Colorado, National Center of Atmospheric Research, 122, 1996.

Bonan, G. B. and Levis, S.: Evaluating aspects of the community land and atmosphere models (CLM3 and CAM3) using a Dynamic Global Vegetation Model, J. Climate, 19, 2290–2301, 2006.

Bonan, G. B., Levis, S., Sitch, S., Vertenstein, M., and Oleson, K. W.: A dynamic global vegetation model for use with climate models: concepts and description of simulated vegetation dynamics, Glob. Change Biol., 9, 1543–1566, 2003.

Bonan, G. B., Lawrence, P. J., Oleson, K. W., Levis, S., Jung, M., Reichstein, M., Lawrence, D. M. and Swenson, S. C.: Improving canopy processes in the Community Land Model version 4 (CLM4) using global flux fields empirically inferred from FLUXNET data, J. Geophys. Res.- Biogeo., 116, G02014, doi:10.1029/2010JG001593, 2011.

Botta, A., Viovy, N., Ciais, P., Friedlingstein, P., and Monfray, P.: A global prognostic scheme of leaf onset using satellite data, Glob. Change Biol., 6, 709–725, 2000.

Bradley, N. L., Leopold, A. C., Ross, J., and Huffaker, W.: Phenological changes reflect climate change in Wisconsin, P. Natl. Acad. Sci. USA, 96, 9701–9704, 1999.

Calvo-Alvarado, J. C., McDowell, N. G., and Waring, R. H.: Allometric relationships predicting foliar biomass and leaf area: sapwood area ratio from tree height in five Costa Rican rain forest species, Tree Physiol., 28, 1601–1608, 2008.

Cannell, M. G. R. and Thornley, J. H. M.: Modelling the components of plant respiration: some guiding principles, Ann. Bot.-London, 85, 45–54, 2000.

Cox, P. M.: Description of the "TRIFFID" Dynamic Global Vegetation Model, London, Hadley Centre, 16, 2001.

Cramer, W., Bondeau, A., Woodward, F. I., Prentice, I. C., Betts, R. A., Brovkin, V., Cox, P. M., Fisher, V., Foley, J. A., Friend, A. D., Kucharik, C., Lomas, M. R., Ramankutty, N., Sitch, S., Smith, B., White, A., and Young-Molling, C.: Global response of terrestrial ecosystem structure and function to CO_2 and climate change: results from six dynamic global vegetation models, Glob. Change Biol., 7, 357–373, 2001.

Defries, R. S., Field, C. B., Fung, I., Justice, C. O., Los, S. O., Matson, P. A., Matthews, E., Mooney, H. A., Potter, C., Prentice, K. C., Sellers, P. J., Townshend, J., Tucker, C. J., Ustin, S. L., and Vitousek, P.: Mapping the land-surface for global atmosphere–biosphere models – toward continuous distributions of vegetations functional-properites, J. Geophys. Res.-Atmos., 100, 20867–20882, 1995.

Del Grosso, S. J., Parton, W. J., Mosier, A. R., Holland, E. A., Pendall, E., Schimel, D. S., and Ojima, D. S.: Modeling soil CO_2 emissions from ecosystems, Biogeochemistry, 73, 71–91, 2005.

Delire, C. and Foley, J. A.: Evaluating the performance of a land Surface/ecosystem model with biophysical measurements from contrasting environments, J. Geophys. Res.-Atmos., 104, 16895–16909, 1999.

Dickinson, R. E., Shaikh, M., Bryant, R., and Graumlich, L.: Interactive canopies for a climate model, Journal of Climate, 11, 2823–2836, 1998.

Dirmeyer, P. A.: Vegetation stress as a feedback mechanism in midlatitude drought, J. Climate, 7, 1463–1483, 1994.

Dragoni, D., Schmid, H. P., Grimmond, C. S. B., and Loescher, H. W.: Uncertainty of annual net ecosystem productivity estimated using eddy covariance flux measurements, J. Geophys. Res.-Atmos., 112, D17102, doi:10.1029/2006JD008149, 2007.

Dunne, J. P., John, J. G., Shevliakova, E., Stouffer, R. J., Krasting, J. P., Malyshev, S. L., Milly, P. C. D., Sentman, L. T., Adcroft, A. J., Cooke, W., Dunne, K. A., Griffies, S. M., Hallberg, R. W., Harrison, M. J., Levy, H., Wittenberg, A. T., Phillips, P. J., and Zadeh, N.: GFDL's ESM2 Global Coupled Climate-Carbon Earth System Models. Part II: Carbon System Formulation and Baseline Simulation Characteristics, J. Climate, 26, 2247–2267, 2013.

Epron, D., Bahn, M., Derrien, D., Lattanzi, F. A., Pumpanen, J., Gessler, A., Hogberg, P., Maillard, P., Dannoura, M., Gerant, D., and Buchmann, N.: Pulse-labelling trees to study

36

carbon allocation dynamics: a review of methods, current knowledge and future prospects, Tree Physiol., 32, 776–798, 2012a.

Epron, D., Laclau, J.-P., Almeida, J. C. R., Gon Balves, J. L. M., Ponton, S., Sette Jr., C. R., Delgado-Rojas, J. S., Bouillet, J.-P., and Nouvellon, A. Y.: Do changes in carbon allocation account for the growth response to potassium and sodium applications in tropical Eucalyptus plantations?, Tree Physiol., 32, 667–679, 2012b.

Falge, E., Baldocchi, D., Tenhunen, J., Aubinet, M., Bakwin, P., Berbigier, P., Bernhofer, C., Burba, G., Clement, R., Davis, K. J., Elbers, J. A., Goldstein, A. H., Grelle, A., Granier, A., Guðmundsson, J., Hollinger, D., Kowalski, A. S., Katul, G., Law, B. E., Malhi, Y., Meyers, T., Monson, R. K., Munger, J. W., Oechel, W., Paw U, K. T., Pilegaard, K., Rannik, Ü., Rebmann, C., Suyker, A., Valentini, R., Wilson, K., and Wofsy, S.: Seasonality of ecosystem respiration and gross primary production as derived from FLUXNET measurements, Agr. Forest Meteorol., 113, 75–95, 2002.

Farquhar, G. and Von Caemmerer, S.: Modeling photosynthetic response to environmental conditions, in: Encyclopedia of Plant Physiol., edited by: Lange, O. L., Nobel, P. S., Os mond, C. B., and Ziegler, H., Springer-Verlag, Berlin, 549–587, 1982.

Farquhar, G. D., Caemmerer, S. V., and Berry, J. A.: A biochemical model of photosynthetic CO_2 assimilation in leaves of C3 species, Planta, 149, 78–90, 1980.

Foley, J. A., Prentice, I. C., Ramankutty, N., Levis, S., Pollard, D., Sitch, S., and Haxeltine, A.: An integrated biosphere model of land surface processes, terrestrial carbon balance, and vegetation dynamics, Global Biogeochem. Cy., 10, 603–628, 1996.

Franklin, O., Johansson, J., Dewar, R. C., Dieckmann, U., McMurtrie, R. E., Brannstrom, A., and Dybzinski, R.: Modeling carbon allocation in trees: a search for principles, Tree Physiol., 32, 648–666, 2012.

Friedlingstein, P., Joel, G., Field, C. B., and Fung, I. Y.: Toward an allocation scheme for global terrestrial carbon models, Glob. Change Biol., 5, 755–770, 1999.

Friedlingstein, P., Cox, P., Betts, R., Bopp, L., Von Bloh, W., Brovkin, V., Cadule, P., Doney, S., Eby, M., Fung, I., Bala, G., John, J., Jones, C., Joos, F., Kato, T., Kawamiya, M., Knorr, W., Lindsay, K., Matthews, H. D., Raddatz, T., Rayner, P., Reick, C., Roeckner, E., Schnitzler, K.- G., Schnur, R., Strassmann, K., Weaver, A. J., Yoshikawa, C., and Zeng, N.:

Climate-carbon cycle feedback analysis: results from the C(4)MIP model intercomparison, J. Climate, 19, 3337–3353, 2006.

Friedlingstein, P., Meinshausen, M., Arora, V. K., Jones, C. D., Anav, A., Liddicoat, S. K., and Knutti, R.: Uncertainties in CMIP5 climate projections due to carbon cycle feedbacks, J. Climate, 27, 511–526, 2014.

Friend, A. D., Arneth, A., Kiang, N. Y., Lomas, M., Ogée, J., Rödenbeck, C., Running, S. W., Santaren, J.-D., Sitch, S., Viovy, N., Woodward, F. I., and Zaele, S.: FLUXNET and modelling the global carbon cycle, Glob. Change Biol., 13, 610–633, 2007.

Fung, I., Doney, S., Lindsay, K., and John, J.: Evolution of carbon sinks in a changing climate, Proc Natl Acad Sci, 102, 11201–11206, 2005.

Goulden, M. L., Munger, J. W., Fan, S. M., Daube, B. C., and Wofsy, S. C.: Exchange of carbon dioxide by a deciduous forest: response to interannual climate variability, Science, 271, 1576–1578, 1996.

Hanninen, H. and Kramer, K.: A framework for modelling the annual cycle of trees in boreal and temperate regions, Silva Fenn., 41, 167–205, 2007.

Hutyra, L. R., Munger, J. W., Saleska, S. R., Gottlieb, E., Daube, B. C., Dunn, A. L., Amaral, D. F., de Camargo, P. B., and Wofsy, S. C.: Seasonal controls on the exchange of carbon and water in an Amazonian rain forest, J. Geophys. Res.-Biogeo., 112, G03008, doi:10.1029/2006JG000365, 2007.

Ilvesniemi, H. and Liu, C.: Biomass distribution in a young Scots pine stand, Boreal Environ. Res., 6, 3–8, 2001.

Jackson, R. B., Canadell, J., Ehleringer, J. R., Mooney, H. A., Sala, A., and Schulze, E. D.: A global analysis of root distributions for terrestrial biomes, Oecologia, 108, 389-411, 1996.

Jolly, W. M. and Running, S. W.: Effects of precipitation and soil water potential on drought deciduous phenology in the Kalahari, Glob. Change Biol., 10, 303–308, 2004.

Jolly, W. M., Nemani, R., and Running, S. W.: A generalized, bioclimatic index to predict foliar phenology in response to climate, Glob. Change Biol., 11, 619–632, 2005.

Keeling, C. D., Chin, J. F. S., and Whorf, T. P.: Increased activity of northern vegetation inferred from atmospheric CO_2 measurements, Nature, 382, 146–149, 1996.

38

Kiang, N. Y.: Savannas and seasonal drought: the landscape-leaf connection through optimal stomatal control, in: Environmental Science, Policy and Management, University of California at Berkeley, Berkeley, 303 pp., 2002.

Kim, Y. and Wang, G. L.: Impact of vegetation feedback on the response of precipitation to antecedent soil moisture anomalies over North America, J. Hydrometeorol., 8, 534–550, 2007.

Kim, Y., Knox, R. G., Longo, M., Medvigy, D., Hutyra, L. R., Pyle, E. H., Wofsy, S. C., Bras, R. L., and Moorcroft, P. R. Seasonal carbon dynamics and water fluxes in an Amazon rainforest, Glob. Change Biol., 18, 1322–1334, 2012.

Kleidon, A. and Mooney, H. A.: A global distribution of biodiversity inferred from climatic constraints: results from a process-based modelling study, Glob. Change Biol., 6, 507–523, 2000.

Koster, R. D., Guo, Z., Dirmeyer, P. A., Yang, R., Mitchell, K., and Puma, M. J.: On the nature of soil moisture in land surface models, J. Climate, 22, 4322–4335, 2009.

Kramer, K., Leinonen, I., and Loustau, D.: The importance of phenology for the evaluation of impact of climate change on growth of boreal, temperate and Mediterranean forests ecosystems: an overview, Int. J. Biometeorol., 44, 67–75, 2000.

Krinner, G., Viovy, N., de Noblet-Ducoudré, N., Ogée, J., Polcher, J., Friedlingstein, P., Ciais, P., Sitch, S., and Prentice, I. C.: A dynamic global vegetation model for studies of the coupled atmosphere–biosphere system, Global Biogeochem. Cy., 19, GB1015, doi:10.1029/2003GB002199, 2005.

Kucharik, C., Barford, C., El Maayar, M., Wofsy, S. C., Monson, R. K., and Baldocchi, D. D.: A multiyear evaluation of a Dynamic Global Vegetation Model at three AmeriFlux forest sites: vegetation structure, phenology, soil temperature, and CO_2 and H_2O vapor exchange, Ecol. Model., 196, 1–31, 2006.

Levis, S. and Bonan, G. B.: Simulating springtime temperature patterns in the community atmosphere model coupled to the community land model using prognostic leaf area, J. Climate, 17, 4531–4540, 2004.

Lockhart, J. A.: An analysis of irreversible plant cell elongation, J. Theor. Biol., 8, 264–275, 1965.

39

Makela, A., Hari, P., Berninger, F., Hanninen, H., and Nikinmaa, E.: Acclimation of photosynthetic capacity in Scots pine to the annual cycle of temperature, Tree Physiol., 24, 369–376, 2004.

Mäkelä, A., Kolari, P., Karimäki, J., Nikinmaa, E., Perämäki, M., and Hari, P.: Modelling five years of weather-driven variation of GPP in a boreal forest, Agr. Forest Meteorol., 139, 382–398, 2006.

Matthews, E.: Global vegetation and land use: new high-resolution data bases for climate studies, Journal of Climate and Applied Meteorology, 22, 474-487, 1983.

Medvigy, D., Walko, R. L., and Avissar, R.,: Modeling interannual variability of the Amazon hydroclimate, Geophys. Res. Lett., 35, L15817, doi:10.1029/2008GL034941, 2008.

Medvigy, D., Wofsy, S. C., Munger, J. W., Hollinger, D. Y., and Moorcroft, P. R.,: Mechanistic scaling of ecosystem function and dynamics in space and time: ecosystem demography model version 2, J. Geophys. Res., 114, G01002, doi:10.1029/2008JG000812, 2009.

Menzel, A.: Trends in phenological phases in Europe between 1951 and 1996, Int. J. Biometeorol., 44, 76–81, 2000.

Mo, X., Chen, J. M., Ju, W., and Black, T. A.: Optimization of ecosystem model parameters through assimilating eddy covariance flux data with an ensemble Kalman filter, Ecol. Model., 217, 157–173, 2008.

Moorcroft, P. R., Hurtt, G. C., and Pacala, S. W.: A method for scaling vegetation dynamics: the ecosystem demography model (ED), Ecol. Monogr., 71, 557–585, 2001.

Ni-Meister,W., Yang,W. Z., and Kiang, N. Y.: A clumped-foliage canopy radiative transfer model for a global dynamic terrestrial ecosystem model, I: Theory, Agr. Forest Meteorol., 150, 881–894, 2010.

Payne, C.: Modification of the nitrogen content and C:N ratio of Sitka spruce timber by kiln and air drying, de Gruyter, Berlin, Allemagne, 2002.

Potter, C. S., Randerson, J. T., Field, C. B., Matson, P. A., Vitousek, P. M., Mooney, H. A., and Klooster, S. A.: Terrestrial ecosystem production: a process model based on global satellite and surface data, Global Biogeochem. Cy., 7, 811–841, 1993.

40

Pumpanen, J., Heinonsalo, J., Rasilo, T., Villemot, J., and Ilvesniemi, H.: The effects of soil and air temperature on CO2 exchange and net biomass accumulation in Norway spruce, Scots pine and silver birch seedlings, Tree Physiol., 32, 724–736, 2012.

Randerson, J. T., Thompson, M. V., Conway, T. J., Fung, I. Y., and Field, C. B.: The contribution of terrestrial sources and sinks to trends in the seasonal cycle of atmospheric carbon dioxide, Global Biogeochemical Cycles, 11, 535-560, 1997.

Randerson, J. T., Hoffman, F. M., Thornton, P. E., Mahowald, N. M., Lindsay, K., Lee, Y. H., Nevison, C. D., Doney, S. C., Bonan, G., Stockli, R., Covey, C., Running, S. W., and Fung, I. Y.: Systematic assessment of terrestrial biogeochemistry in coupled climate-carbon models, Glob. Change Biol., 15, 2462–2484, 2009.

Reich, P. B., Wright, I. J., and Lusk, C. H.: Predicting leaf physiology from simple plant and climate attributes: a global GLOPNET analysis, Ecol. Appl., 17, 1982–1988, 2007.

Repo, T., Makela, A., and Hanninen, H.: Modelling frost resistance of trees, in: Modelling to Understand Forest Function, edited by: Jozefek, H., Silva Carelica, 61–74, 1990.

Richardson, A. D., Anderson, R. S., Arain, A. M., Barr, A. L. A. N. G., Bohrer, G., Chen, G., Chen, J. M., Ciais, P., Davis, K. J., Desai, A. R., Dietze, M. C., Dragoni, D., Garrity, S. R., Gough, C. M., Grant, R., Hollinger, D. Y., Margolis, H. A. N. K. A., McCaughey, H., Migliavacca, M., Monson, R. K., Munger, W. J., Poulter, B., Raczka, B. M., Ricciuto, D. M., Sahoo, A. K., Schaefer, K. E. V. I. N., Tian, H., Vargas, R., Verbeeck, H., Xiao, J., and Xue, Y.: Terrestrial biosphere models need better representation of vegetation phenology: results from the North American Carbon Program Site Synthesis, Glob. Change Biol., 18, 566–584, 2012.

Richardson, A. D., Keenan, T. F., Migliavacca, M., Ryu, Y., Sonnentag, O., and Toomey, M.: Climate change, phenology, and phenological control of vegetation feedbacks to the climate system, Agr. Forest Meteorol., 169, 156–173, 2013.

Rodriguez-Iturbe, I., Porporato, A., Laio, F., and Ridolfi, L.: Plants in water-controlled ecosystems: active role in hydrologic processes and responses to water stress, I. Scope and general outline, Adv. Water Resour., 24, 695–705, 2001.

Rosenzweig, C. and Abramopoulos, F.: Land-surface model development for the GISS GCM, J. Climate, 10, 2040–2054, 1997.

Sala, A., Woodruff, D. R., and Meinzer, F. C.: Carbon dynamics in trees: feast or famine?, Tree Physiol., 32, 764–775, 2012.

Schmid, H. P., Grimmond, C. S. B., Cropley, F., Offerle, B., and Su, H. B.: Measurements of CO_2 and energy fluxes over a mixed hardwood forest in the mid-western United States, Agr. Forest Meteorol., 103, 357–374, 2000.

Schmidt, G. A., Ruedy, R., Hansen, J. E., Aleinov, I., Bell, N., Bauer, M., Bauer, S., Cairns, B., Canuto, V., Cheng, Y., Del Genio, A., Faluvegi, G., Friend, A. D., Hall, T. M., Hu, Y., Kelley, M., Kiang, N. Y., Koch, D., Lacis, A. A., Lerner, J., Lo, K. K., Miller, R. L., Nazarenko, L., Oinas, V., Perlwitz, J. P., Perlwitz, J., Rind, D., Romanou, A., Russell, G. L., Sato, M., Shindell, D. T., Stone, P. H., Sun, S., Tausnev, N., Thresher, D., and Yao, M.-S.: Present day atmospheric simulations using GISS ModelE: comparison to in-situ, satellite and reanalysis data, J. Climate, 19, 153–192, doi:10.1175/JCLI3612.1, 2006.

Schmidt, G. A., Kelley, M., Nazarenko, L., Ruedy, R., Russell, G. L., Aleinov, I., Bauer, M., Bauer, S. E., Bhat, M. K., Bleck, R., Canuto, V., Chen, Y.-H., Cheng, Y., Clune, T. L., Del Genio, A., de Fainchtein, R., Faluvegi, G., Hansen, J. E., Healy, R. J., Kiang, N. Y., Koch, D., Lacis, A. A., LeGrande, A. N., Lerner, J., Lo, K. K., Matthews, E. E., Menon, S., Miller, R. L., Oinas, V., Oloso, A. O., Perlwitz, J. P., Puma, M. J., Putman, W. M., Rind, D., Romanou, A., Sato, M., Shindell, D. T., Sun, S., Syed, R. A., Tausnev, N., Tsigaridis, K., Unger, N., Voulgarakis, A., Yao, M.-S., and Zhang, J.: Configuration and assessment of the GISS ModelE2 contributions to the CMIP5 archive, J. Adv. Model. Earth Syst., 6, 141–184, 2014.

Schneider, R., Berninger, F., Ung, C. H., Makela, A., Swift, D. E., and Zhang, S. Y., Within crown variation in the relationship between foliage biomass and sapwood area in jack pine, Tree Physiol., 31, 22–29, 2011.

Sitch, S., Smith, B., Prentice, I.C., Arneth, A., Bondeau, A., Cramer, W., Kaplan, J., Levis, S., Lucht, W., Sykes, M., Thonicke, K., and Venevsky, S: Evaluation of ecosystem dynamics, plant geography and terrestrial carbon cycling in the LPJ dynamic global vegetation model, Glob. Change Biol., 9, 161–185, 2003.

Stephens, B. B., Gurney, K. R., Tans, P. P., Sweeney, C., Peters, W., Bruhwiler, L., Ciais, P., Ramonet, M., Bousquet, P., Nakazawa, T., Aoki, S., Machida, T., Inoue, G., Vinnichenko, N., Lloyd, J., Jordan, A., Heimann, M., Shibistova, O., Langenfelds, R., Steele, L. P., Francey, T.,

and Denning, A. S.: Weak northern and strong tropical land carbon uptake from vertical profiles of atmospheric CO2, Science, 316, 1732–1735, 2007.

Stöckli, R. and Vidale, P. L.: European plant phenology and climate as seen in a 20 year AVHRR land-surface parameter dataset, Int. J. Remote Sens., 25, 3303–3330, 2004.

Stöckli, R., Lawrence, D. M., Niu, G.-Y., Oleson, K. W., Thornton, P. E., Yang, Z.-L., Bonan, G. B., Denning, A. S., and Running, S. W.: Use of FLUXNET in the community land model development, J. Geophys. Res.-Biogeo., 113, G01025, doi:10.1029/2007JG000562, 2008.

Stöckli, R., Rutishauser, T., Baker, I., Liniger, M. A., and Denning, A. S.: A global reanalysis of vegetation phenology, J. Geophys. Res.-Biogeo., 116, G03020, doi:10.1029/2010JG001545, 2011.

Tang, J. W. and Baldocchi, D. D.: Spatial–temporal variation in soil respiration in an oak-grass savanna ecosystem in California and its partitioning into autotrophic and heterotrophic components, Biogeochemistry, 73, 183–207, 2005.

Tang, J. W., Baldocchi, D. D., and Xu, L.: Tree photosynthesis modulates soil respiration on a diurnal time scale, Glob. Change Biol., 11, 1298–1304, 2005.

Thompson, M. V., Randerson, J. T., Malmström, C. M., and Field, C. B.: Change in net primary production and heterotrophic respiration: How much is necessary to sustain the terrestrial carbon sink?, Global Biogeochemical Cycles, 10, 711-726, 1996.

Urbanski, S., Barford, C., Wofsy, S., Kucharik, C., Pyle, E., Budney, J., McKain, K., Fitzjarrald, D., Czikowsky, M., and Munger, J. W.: Factors controlling CO2 exchange on timescales from hourly to decadal at Harvard Forest, J. Geophys. Res.-Biogeo., 112, G02020, doi:10.1029/2006JG000293, 2007.

van der Tol, C., Berry, J. A., Campbell, P. K. E., and Rascher, U.: Models of fluorescence and photosynthesis for interpreting measurements of solar-induced chlorophyll fluorescence, J. Geophys. Res.-Biogeo., 119, 2312–2327, 2014.

Wang, Y. P., Baldocchi, D., Leuning, R., Falge, E., and Vesala, T.: Estimating parameters in a land-surface model by applying nonlinear inversion to eddy covariance flux measurements from eight FLUXNET sites, Glob. Change Biol., 13, 652–670, 2007.

Wei, J., Dickinson, R. E., and Zeng, N.: Climate variability in a simple model of warm climate land–atmosphere interaction, J. Geophys. Res.-Biogeo., 111, G03009, doi:10.1029/2005JG000096, 2006.

Welp, L. R., Keeling, R. F., Meijer, H. A. J., Bollenbacher, A. F., Piper, S. C., Yoshimura, K., Francey, R. J., Allison, C. E., and Wahlen, M.: Interannual variability in the oxygen isotopes of atmospheric CO2 driven by El Niño, Nature, 477, 579–582, 2011.

White, M. A., Thornton, P. E., and Runnning, S. W.: A continental phenology model for monitoring vegetation responses to interannual climatic variability, Global Biogeochem. Cy., 11, 217–234, 1997.

Wilson, K., Goldstein, A., Falge, E., Aubinet, M., Baldocchi, M., Berbigier, P., Bernhofer, C., Ceulemans, R., Dolman, H., Field, C., Grelle, A., Ibrom, A., Law, B. E., Kowalski, A., Meyers, T., Moncrieff, J., Monson, R., Oechel, W., Tenhunen, J., Verma, S., and Valentini, R.: Energy balance closure at FLUXNET sites, Agr. Forest Meteorol., 113, 223–243, 2002.

Xu, L. and Baldocchi, D. D.: Seasonal variation in carbon dioxide exchange over a Mediterranean annual grassland in California, Agr. Forest Meteorol., 123, 79–96, 2004.

Xue, Y. K., Fennessy, M. J., and Sellers, P. J.: Impact of vegetation properties on US summer weather prediction, J. Geophys. Res.-Atmos., 101, 7419–7430, 1996.

Yang, W., Ni-Meister, W., Kiang, N. Y., Moorcroft, P. R., Strahler, A. H., and Oliphant, A.: A clumped-foliage canopy radiative transfer model for a Global Dynamic Terrestrial Ecosystem Model II: comparison to measurements, Agr. Forest Meteorol., 150, 895–907, 2010.

Zhang, X. Y., Tarpley, D., and Sullivan, J. T.: Diverse responses of vegetation phenology to a warming climate, Geophys. Res. Lett., 34, L19405, doi:10.1029/2007GL031447, 2007.

Yeonjoo 9/7/15 10:50 AM

Deleted: Abramopoulos, F., Rosenzweig, C. and Choudhury, B.J.: Improved ground hydrology calculations for global climate models (GCMs): soil water movement and evapotranspiration, Journal of Climate, 1, 921-941, 1988. ... [38]

1   Table 1. Plant Functional Types (PFT) in Ent.

Number	Plant Function Type
1	Evergreen broadleaf early successional
2	Evergreen broadleaf late successional
3	Evergreen needleleaf early successional
4	Evergreen needleleaf late successional
5	Cold deciduous broadleaf early successional
6	Cold deciduous broadleaf late successional
7	Drought deciduous broadleaf
8	Deciduous needleleaf
9	Cold adapted shrub
10	Arid adapted shrub
11	C3 grass perennial
12	C4 grass
13	C3 grass annual
14	Arctic C3 grass
15	C3 crops
16	C4 crops
17	Crops broadleaf woody

2

3

Table 2. Parameters in phenology submodel.

Parameters	Values	Eq. #	References
GDD_{int}	-68		
GDD_{slop}	638	(3)	Botta et al. (2000)
GDD_{multi}	-0.01		
GDD_{length}	200	(4)	Derived from observations at MMSF
T_{max}	15		
T_{min}	5	(5)	Adjusted based on Jolly et al. (2005)
ld_{max}	540		
ld_{max}	660		
$SGDD_{crit}$	100 for arctic C3 grass; 400 for C3 grass; 1400 for C4 grass;	(6)	Arctic C3 grass derived from observations at Barrow, AK C3 annual grass from White et al. (1997)
$SGDD_{length}$	50		
TS_{max}	0	(7)	Derived from observations at Tonzi and Vaira
TS_{min}	-5		
β_{max}	0.4 for both woody and herbaceous		Derived from observations at Tonzi
β_{min}	0.0 for woody; 0.2 for herbaceous	(8)	
β_{resis}	0.25 for woody; 1.0 for herbaceous		
a	1	(9)	
b	0		Makela et al. (2006)
τ	125 hr	(10)	
T_0	-5.9°C		
$S_{h,max}$	16.8°C	(11)	Derived from observations at Hyytiala

46

Table 3. Site descriptions.

	Morgan Monroe State Forest	Harvard Forest	Vaira Ranch	Tonzi Ranch	Hyytiala
Short name	MMS	Ha1	Var	Ton	Hyy
Location	Indiana, USA	Massachusetts, USA	California, USA	California, USA	Hyytiala, Finland
Coordinates	39.32°N, 86.41°W	42.54°N, 72.17°W	38.41°N, 120.95°W	38.43°N, 120.97°W	61.85°N, 24.29°W
Primary reference	Schmid et al. (2000)	Urbanski et al. (2007)	Xu and Baldocchi (2004)	Baldocchi et al. (2004)	Makela et al. (2004)
Data website	http://ameriflux.ornl.gov/fullsiteinfo.php?sid=48	http://ameriflux.ornl.gov/fullsiteinfo.php?sid=50	http://ameriflux.ornl.gov/fullsiteinfo.php?sid=30	http://ameriflux.ornl.gov/fullsiteinfo.php?sid=29	http://gaia.agraria.unitus.it/home/site-details?id=117
Dominant Species	Sugar maple, Tulip poplar	Red oak, Red maple	Purple false brome	Overstory: Blue oak, Understory: Purple false brome	Scots pine, Norway spruce
Ent PFT	6-cold deciduous broadleaf l.s.	5-cold deciduous broadleaf e.s.	13-annual grass	7-drought deciduous Broadleaf & 13-annual grass	4-evergreen needleleaf
Simulation Period	1 Jan 2002 − 31Dec 2006	1 Jan 1994 − 31Dec 2002	1 Jan 2002 − 31Dec 2002	1 Jan 2002 − 31Dec 2002	1 Jan 1998 − 31Dec 1998
Experiments	LSM-oveg LSM-dveg	LSM-oveg LSM-dveg	Ent-oveg Ent-dveg LSM-oveg LSM-dveg	Ent-oveg Ent-dveg LSM-oveg LSM-dveg	Ent-oveg Ent-dveg LSM-oveg LSM-dveg

1.1

Table 4. Types of experiments.

	Soil state (moisture and temperature)	Vegetation phenology
Ent-dveg	Prescribed with observation (Ent-standalone)	Prognostic LAI (dynamic "active biomass" phenology)
Ent-oveg	Prescribed with observation (Ent-standalone)	Prescribed with observed LAI
LSM-dveg	Prognostic (Ent-LSM coupled)	Prognostic LAI
LSM-oveg	Prognostic (Ent-LSM coupled)	Prescribed with observed LAI

Table 5. Correlation coefficients and RMSEs of LAI-based phenological dates between simulations and observations.

Site	Spring Phenology						Fall Phenology					
	20% LAI		50% LAI		80% LAI		80% LAI		50% LAI		20% LAI	
	R	RMSE	R	RMSE	R	RMSE	R	RMSE	R	RMSE	R	RMSE
MMS (2002-2006)	0.80	3.65	0.36	6.75	0.67	16.44	0.20	27.95	0.46	19.65	0.49	7.67
Ha1 (1994-2002)	0.44	5.71	0.85	3.00	0.44	9.18	0.55	9.91	0.04	15.09	-0.56	17.52

Table 6. Correlation coefficients and RMSEs of hourly and daily fluxes between simulations and observations.

Site	Years		NEP (μmol/m²/s)				ET (mm/s)			
			Hourly		Daily		Hourly		Daily	
			R	RMSE	R	RMSE	R	RMSE	R	RMSE
MMS	2002 -2006	LSM-dveg	0.86	3.67	0.91	1.31	0.80	67.89	0.85	32.82
		LSM-oveg	0.88	3.59	0.94	1.04	0.79	66.62	0.85	32.12
Ha1	1994 -2002	LSM-dveg	0.89	3.03	0.85	1.70	0.79	45.25	0.82	22.46
		LSM-oveg	0.92	2.72	0.92	1.36	0.74	52.12	0.72	29.14
Var	2002	Ent-dveg	0.74	2.92	0.57	1.41	-	-	-	-
		Ent-oveg	0.76	2.81	0.55	1.60	-	-	-	-
		LSM-dveg	0.70	2.57	0.75	1.16	0.84	25.37	0.83	13.46
		LSM-oveg	0.84	2.34	0.72	1.54	0.91	25.73	0.93	11.36
Ton	2002	Ent-dveg	0.42	3.96	0.36	1.51	-	-	-	-
		Ent-oveg	0.44	3.94	0.43	1.50	-	-	-	-
		LSM-dveg	0.41	4.06	0.53	1.37	0.77	5.38	0.83	14.42
		LSM-oveg	0.42	3.99	0.50	1.41	0.76	35.59	0.84	14.40
Hyy	1998	Ent-dveg	0.79	2.63	0.71	1.25	-	-	-	-
		Ent-oveg	0.77	2.90	0.68	1.35	-	-	-	-
		LSM-dveg	0.92	1.66	0.86	0.82	0.87	19.37	0.93	7.89
		LSM-oveg	0.90	1.89	0.82	0.92	0.87	19.30	0.94	7.88

Appendix Table A1. Plant functional type parameters for root density distributions.

	Ent plant functional type															
	Evergreen broad		Evergreen needle		Cold-deciduous broad		drought broad	decidciduous needle	shrub cold	shrub arid	grass				crop herb	crop tree
PET	1	2	3	4	5	6	7	8	9	10	11	12	13	14	15	16
a	1.1	1.1	0.25	0.25	0.25	0.25	0.25	0.25	0.8	0.8	0.9	0.9	0.9	0.9	0.9	0.25
b	0.4	0.4	2.0	2.0	2.0	2.0	2.0	2.0	0.4	0.4	0.9	0.9	0.9	0.9	0.9	2.0

1　Appendix Table B1. Values of C pool parameters: cnratio – C:N ratio of all 12 C pools (used

2　only to calculate N pools); $annk_{soil}$ – inverse of turnover times of all 9 soil C pools (yr^{-1}).

Pool	C:N ratio[1]	$annk_{soil}$[2]	~turnover time
Leaf	30	--	(lrage) See
Root	130	--	(lrage)
Wood	55	--	(woodage)
Surfmet	30	14.8	25 d
Surfstr	50	3.9	94 d
Soilmet	25	18.5	20 d
Soilstr	50	4.9	74 d
CWD	135	0.2424	4.1 yr
Surfmic	12.5	6	60 d
Soilmic	12.5	7.3	50 d
Slow	12.5	0.2	5 yr
Passive	8.5	0.002	500 yr

3　[1]from original CASA code (Potter et al., 1993)

4　[2]from CASA' code (Doney et al., 2006)

52

Appendix Table B2. Values of respiration pathway coefficients: eff – microbial respiration transfer efficiencies for all 14 pathways; frac_donor – additional respiration efficiencies (both unitless)

Pathway[1]	eff[1]	frac_donor[2]
1	0.45	0.003+(0.009*clay frac)
2	0.45	1−frac_donor(1)
3	0.4	1
4	0.4	1−structurallignin(PFT)[3]
5	0.7	structurallignin(PFT)
6	0.45	1
7	0.45	1−structurallignin(PFT)
8	0.7	structurallignin(PFT)
9	0.4	1−woodligninfrac[3]
10	0.7	woodligninfrac
11	0.4	1
12	0.85-[0.68*(silt+sand fracs)]	0.003+(0.032*clay frac)
13	0.85-[0.68*(silt+sand fracs)]	1−frac_donor(12)
14	0.45	1

[1]from CASA code (Potter et al., 1993) for 1−3, others from CASA' code (Doney et al., 2006) **double check which from which code**

[2]from original CASA code (Potter et al., 1993)

[3]derived litter coefficients in both CASA and CASA' codes

53

Appendix Table D1. Biophysics parameters for Fluxnet sites in this study.

Variable	Definition	Unit	PFT4 Hyy	PFT5 Ha1	PFT6 MMS	PFT7 Ton (oak)	PFT13 Var & Ton (grass)
P_{st}	Pst - photosynthetic pathway	-	C3	C3	C3	C3	C3
PAR_{absorb}	Leaf PAR absorbance	-	0.93	0.90	0.90	0.90	0.86
V_{cmax}[1]	Maximum photosynthetic capacity	$\mu mol\ m^{-2}\ s^{-1}$	43.0[2]	60.0[2]	51.0[3]	56.4[4]	50.1[4]
m	Slope of Ball-Berry stomatal conductance equations	-	9.0	9.0	9.0	9.0	11.0
b	Intercept of Ball-Berry stomatal conductance equation	$\mu mol\ m^{-2}\ s^{-1}$	0.002	0.002	0.002	0.002	0.008

[1]For all these plant functional types there is a large range of values, as well as large variation within a single site and single plant. We therefore have chosen literature values for the Fluxnet sites where available, and tuned the value within the literature range for the site.

[2]Oleson et al. (2004)

[3]Wilson et al. (2001)

[4]Wang et al. (2007)

1 Appendix Table D2. Biogeochemical and phenological parameters for Fluxnet sites in this study.

Variable	Defintion	Unit	PFT4 Hyy	PFT5 Ha1	PFT6 MMS	PFT7 Ton (oak)	PFT13 Var & Ton (grass)
leaftype	Leaf type	-	needle	broad	broad	broad	grass
h_{wilt}	Wilting point	m	-153.0	-500.0	-500.0	-500.0	-2030.0
S_*	Soil moisture stress onset point (fraction of soil volumetric saturation)	-	0.50	0.50	50.0	0.34	0.65
s_{wilt}	Wilting point (fraction of soil volumetric saturation)	-	0.25	0.29	0.29	0.28	0.27
sla	Specific leaf area	m^2_{leaf}/kgC_{leaf}	9.5	34.5	34.0	8.3	21.6
r	Respiration parameter	-	1.2	0.6	0.6	0.5	1.2
lrage	Leaf and root litter age	years	4.0	1.2	0.75	1.2	1.5
woodage	Stem litter age	years	42.0	58.0	58.0	245.0	UNDEF
lit_C2N	Litter C:N ratio	-	80.0	57.0	57.0	60.0	50.0
lignin	Lignin content		0.25	0.2	0.3	0.2	0.1
croot_ratio	Coarse roots:woody stem mass ratio	-	0.184	0.093	0.093	0.153	0.0
phenotype	Phenological type	-	Cold deciduous	Cold deciduous	Cold deciduous	Drought deciduous	Annual
b1Cf	Parameter 1 for allometric relation between DBH and foliage carbon	-	0.045	0.024	0.017	0.0296	0.0800
b2Cf	Parameter 2 for allometric relation between DBH	-	1.683	1.860	1.731	1.560	1.000

55

	and foliage carbon						
b1Cd	Parameter 1 for allometric relation between DBH and structural carbon	-	0.1617	0.148	0.235	0.0621	0.00001
b2Cd	Parameter 2 for allometric relation between DBH and structural carbon	-	2.1536	2.411	2.252	2.306	1.000
b1Ht	Parameter 1 for allometric relation between DBH and height	-	22.79	25.18	23.39	34.62	0.4778
b2Ht	Parameter 2 for allometric relation between DBH and height	-	-0.0445	-0.0496	-0.054	-0.02321	-0.75

1

2   Figure 1. Schematic diagram of the Ent model.

3
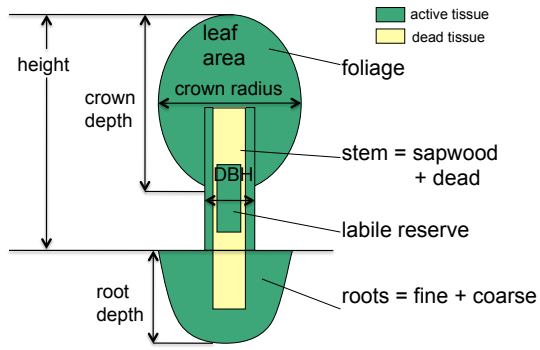
Figure 2. Ent individual plant biomass pools and geometry. Herbaceous plants exclude woody tissue.
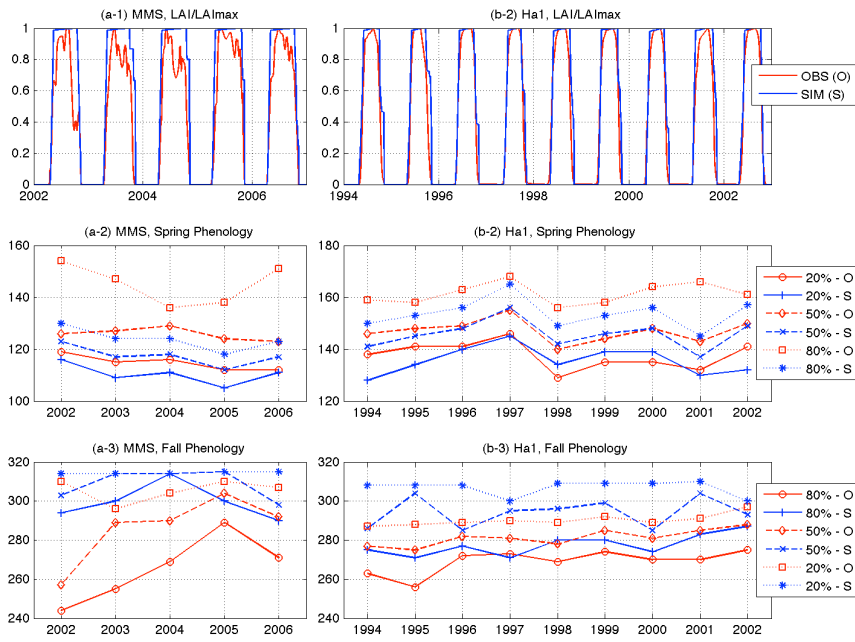
Figure 3. Daily simulated (S) and observed (O) phenology: (top) LAI/LAImax (middle) phenological dates (day of year) for spring leaf-out at percent of maximum; and (bottom) phenological dates (day of year) for fall senescence in MMSF and Harvard Forest. These results show good simulated timing of initial leaf-out and final senescence, but lack of the gradual rate of these, such that maximum leaf-out occurs too soon, and period of peak growth is too long. The gradual behavior could be simulated through a rate constraint.
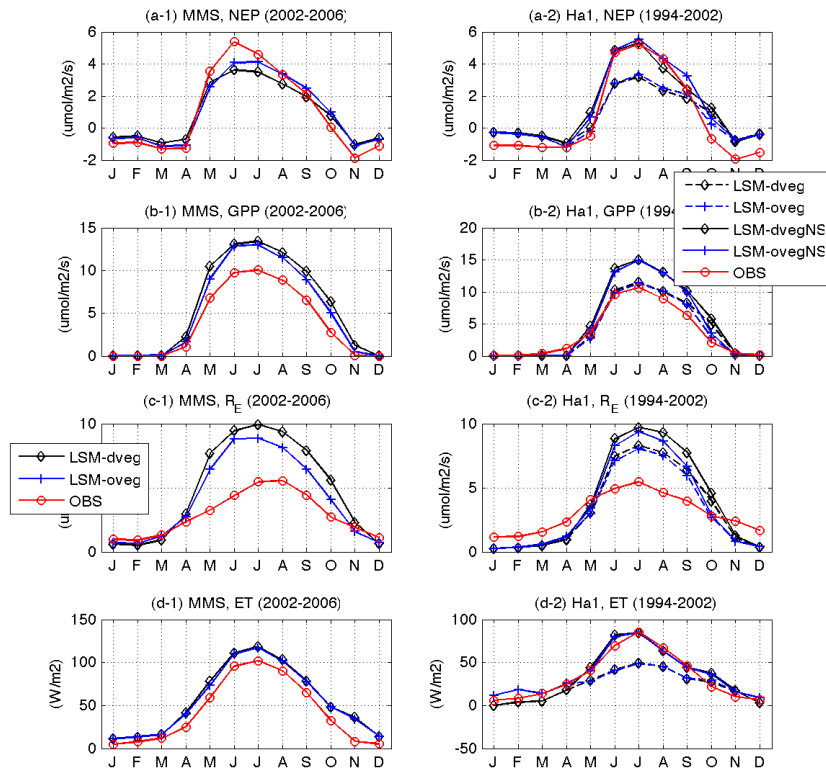
Figure 4. Average monthly fluxes in MMSF for 2002-2006 and Harvard Forest for 1994-2002: (a) NEP, (b) GPP, (c) R_E and (d) ET.

1

2
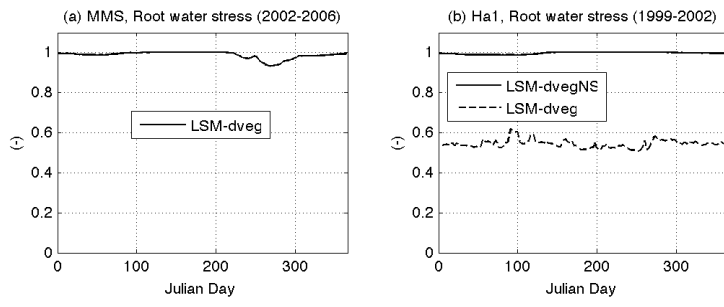
3   Figure 5. Daily root water stress factor in (a) MMSF for 2002-2006 and (b) Harvard Forest

4   for 1994-2002.

5

61
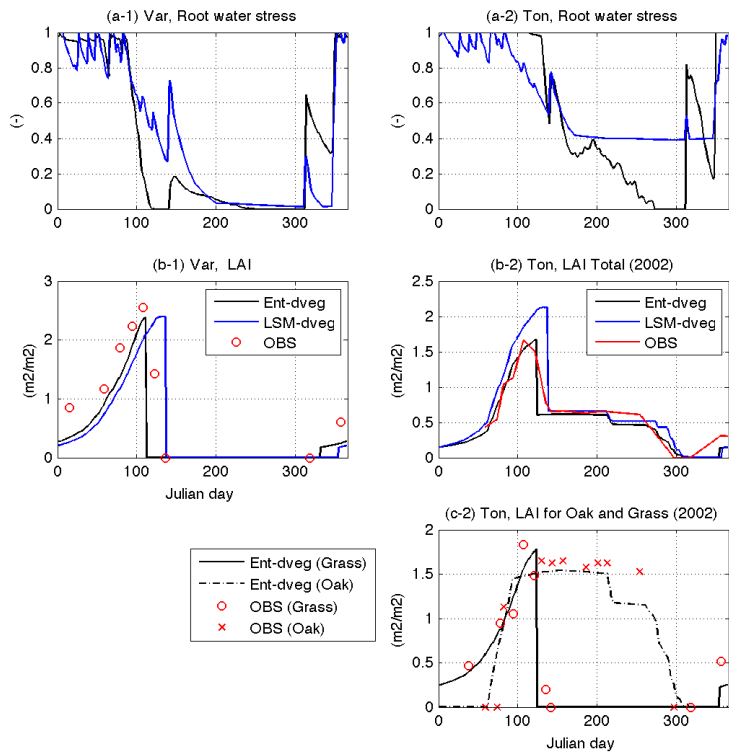
Figure 6.   (a) Daily root water stress and (b-c) daily LAI in Vaira and Tonzi Ranches for 2002.

1

2
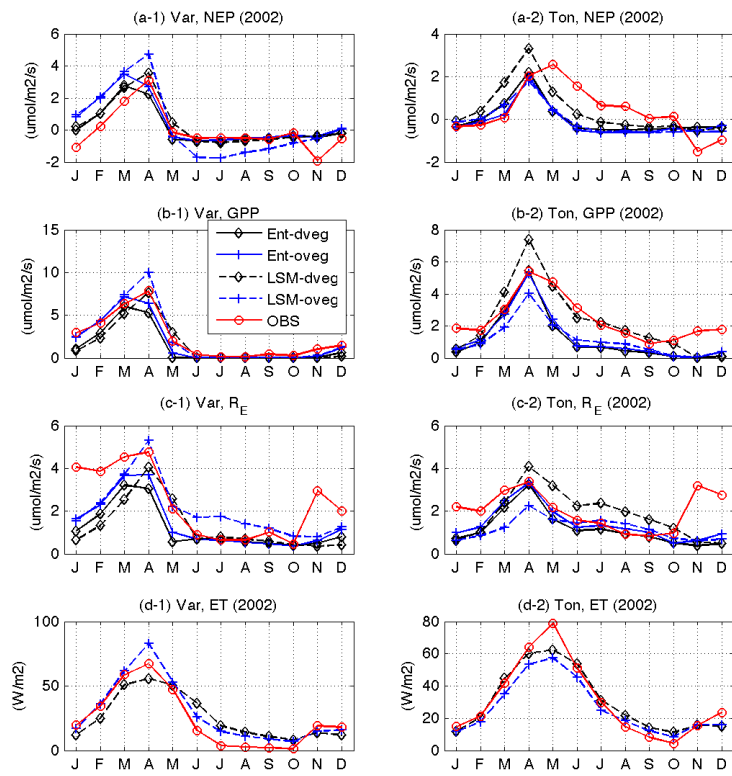
3   Figure 7. Monthly fluxes in Vaira and Tonzi Ranches for 2002: (a) NEP, (b) GPP, (c) R_E and

4   (d) ET.

5
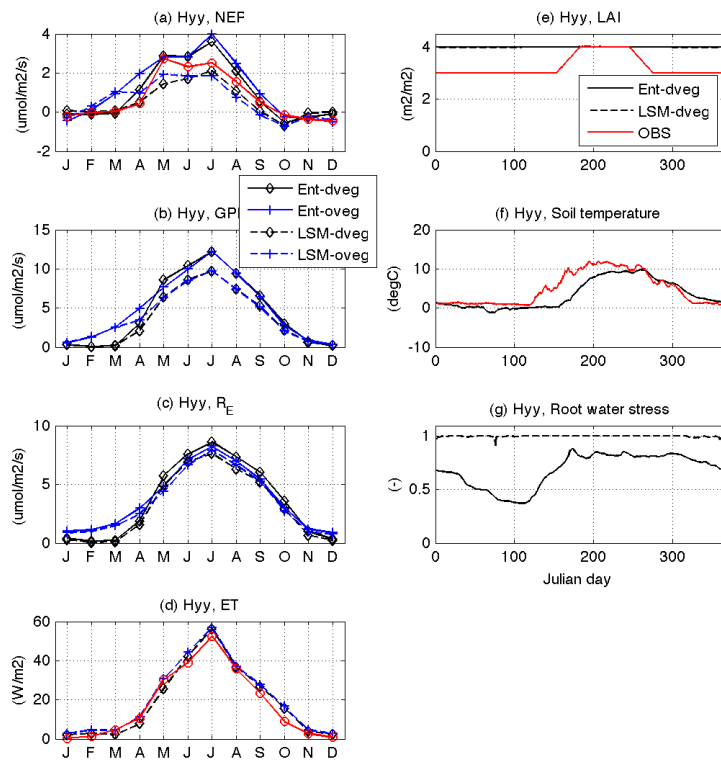
Figure 8. Monthly fluxes and daily states in Hyytiala for 1998: (a) NEP, (b) GPP, (c) RE, (d) ET, (e) LAI, (f) soil temperature and (g) root water stress. Here the observed LAI is assumed based on personal communication with the site investigator, Pasi Kolari.

1
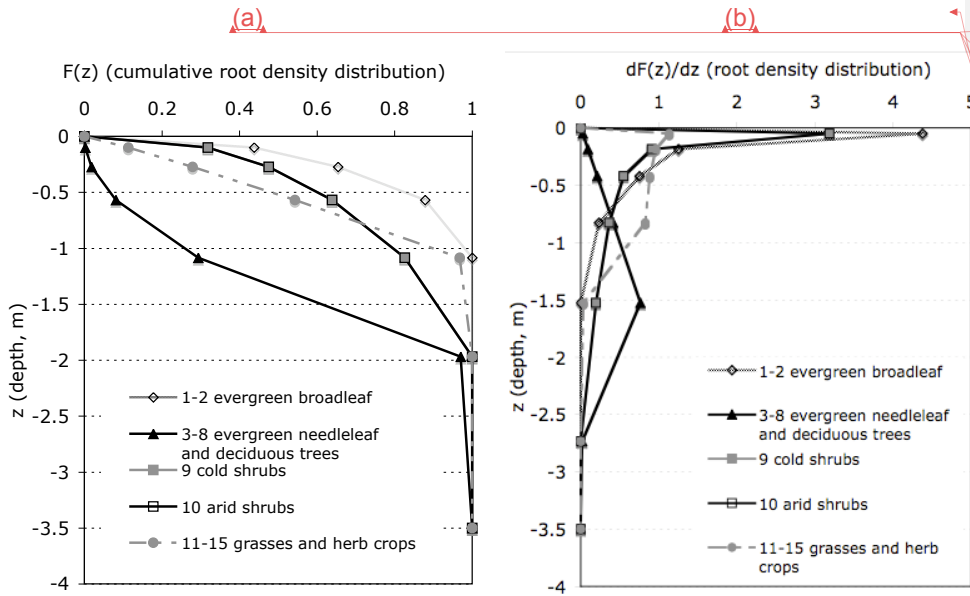
(a) (b)

F(z) (cumulative root density distribution)

dF(z)/dz (root density distribution)

2 Appendix Figure A1. (a) Cumulative root density profile distributions and (b) probability

3 density distributions in the EntTBM, modified from (Rosenzweig and Abramopoulos 1997),

4 by soil depth increments of the NASA GISS GCM land surface model.

5

Appendix Figure B1. Schematic diagram of soil biogeochemistry submodel of Ent (showing 9 soil C pools only; modified from Potter et al., 1993). Surfstr – surface structural pool; Surfmet – surface metabolic pool; Soilmet – soil metabolic pool (fastest to decompose; 20-day turnover time); Soilstr – soil structural pool; Surfmic – surface microbial pool; Soilmic – soil microbial pool; Slow – slowly decomposing pool; Passive – very slowly decomposing pool (500-yr turnover time). All pools except for the 3 surf*** pools are assumed to be present in the 2 lower soil layers in addition to the top layer.

(a)

(b)

Appendix Figure B2. (a) Temperature responses of soil respiration in Del Grosso et al. (2005), CASA', and Ent's piece-wise linear response and (b) moisture response of soil respiration in Del Grosso et al. (2005), CASA', and Ent for grassland (Vaira Ranch) soil texture.